

HPCR: Holistic Proxy-based Contrastive Replay for Online Continual Learning

Huiwei Lin, *Graduate Student Member, IEEE*, Shanshan Feng, Baoquan Zhang, Xutao Li,
Yew-soon Ong, *Fellow, IEEE*, Yunming Ye

Abstract—Online continual learning (OCL) aims to continuously learn new data from a single pass over the online data stream. It generally suffers from the catastrophic forgetting issue. Existing replay-based methods effectively alleviate this issue by replaying part of old data in a proxy-based or contrastive-based replay manner. In this paper, we conduct a comprehensive analysis of these two replay manners and find they can be complementary. Inspired by this finding, we propose a novel replay-based method called proxy-based contrastive replay (PCR), which replaces anchor-to-sample pairs with anchor-to-proxy pairs in the contrastive-based loss to alleviate the phenomenon of forgetting. Based on PCR, we further develop a more advanced method named holistic proxy-based contrastive replay (HPCR), which consists of three components. The contrastive component conditionally incorporates anchor-to-sample pairs to PCR, learning more fine-grained semantic information with a large training batch. The second is a temperature component that decouples the temperature coefficient into two parts based on their impacts on the gradient and sets different values for them to learn more novel knowledge. The third is a distillation component that constrains the learning process to keep more historical knowledge. Experiments on four datasets consistently demonstrate the superiority of HPCR over various state-of-the-art methods.

Index Terms—Online Continual Learning, Catastrophic Forgetting, Deep Metric Learning, Image Classification.

1 INTRODUCTION

ONLINE continual learning (OCL) is a special scenario of continual learning [1]. Taking the problem of classification [2] as an example, its goal is to learn a model that can achieve knowledge accumulation of new classes without forgetting information learned from old classes. In the meantime, the samples of a continuously non-stationary data stream are accessed only once during the learning process. At present, catastrophic forgetting (CF) [3] is the main problem of continual learning. It is associated with the phenomenon that the model suffers a significant performance drop for old classes when learning new classes [4]. The main reason is the historical knowledge of old data would be overwritten as the novel information of new data by the real-time changing distribution [5].

Among all types of methods proposed for continual learning, the replay-based methods have shown superior performance for OCL [6]. In this family of methods [7], [8],

part of previous samples are saved in an episodic memory buffer and then used to learn together with current samples. While training, the number of previous samples in the fixed buffer is much less than the number of current samples in the data stream. Hence, how to efficiently replay limited samples is the key to overcoming the forgetting problem.

In general, there are two ways to replay. The first is the proxy-based replay manner, which is to replay by using the proxy-based loss function and softmax classifier. As shown in Figure 1(a), it calculates similarities between each anchor and all proxies belonging to C classes. Here, a proxy can be regarded as the representative of a class [9], and the anchor is one of the samples in a training batch. The second is the contrastive-based replay manner that replays by using the contrastive-based loss function and nearest class mean (NCM) classifier [10]. Shown as Figure 1(b), it computes similarities between each anchor and all N samples in the same training batch. Although these two manners are effective, they have their corresponding limitations. The former is subjected to the “bias” issue caused by class imbalance, tending to classify most samples of old classes into new classes. The latter is unstable and hard to converge in the training process, requiring a large number of samples.

In this work, we comprehensively analyze their characteristics and find that coupling them can achieve complementary advantages. On the one hand, the proxy-based replay manner focuses on exploring anchor-to-proxy relations for all learned classes, where some fine-grained semantic information will be lost. However, it enables fast and reliable convergence with the help of proxies, which can overcome the problems of being unstable and hard to converge in the contrastive-based replay manner. On the other hand, the contrastive-based replay manner mainly mines the knowl-

- Huiwei Lin, Baoquan Zhang, Xutao Li, Yunming Ye are with the Department of Computer Science, Harbin Institute of Technology, Shenzhen 518055, China, and also with Shenzhen Key Laboratory of Internet Information Collaboration, Shenzhen 518055, China. E-mail: linhuiwei@stu.hit.edu.cn, baoquanzhang@yeah.net, lixutao@hit.edu.cn, yeyunming@hit.edu.cn
- Shanshan Feng is with Centre for Frontier AI Research, Institute of High Performance Computing, A*STAR, Singapore. E-mail: victor_fengss@foxmail.com.
- Yew-Soon Ong is with the Agency for Science, Technology and Research (A*STAR), Singapore and also with the School of Computer Science and Engineering, Nanyang Technological University, Singapore. E-mail: ongyewsoon@hpc.a-star.edu.sg; asyong@ntu.edu.sg.

Manuscript received 1 Apr. 2023; revised 1 Apr. 2023; accepted 1 Apr. 2023.
Date of publication 28 Apr. 2023; date of current version 4 Apr. 2023.
(Corresponding authors: Yunming Ye and Shanshan Feng.)
Recommended for acceptance by XXXX.
Digital Object Identifier XX.XXXX/TPAMI.20XX.XXXXXXX

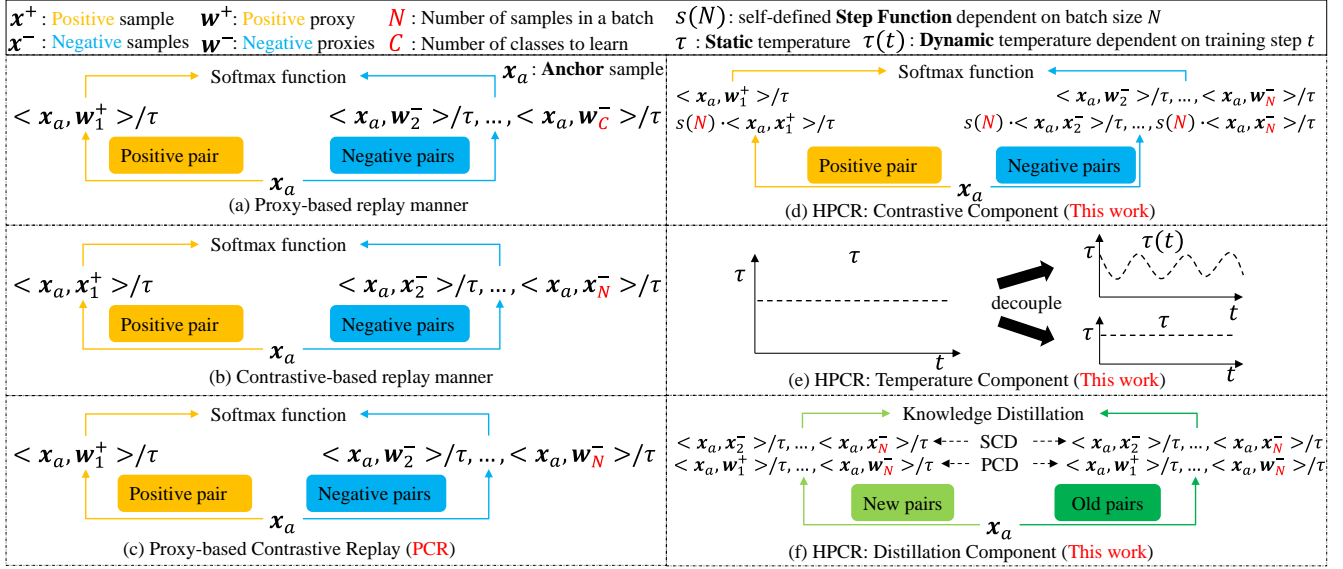


Fig. 1. Illustration of our work. (a) The example of proxy-based replay manner. For each anchor sample, it calculates similarities of all anchor-to-proxy pairs. (b) The example of contrastive-based replay manner. For each anchor sample, it calculates similarities of all anchor-to-sample pairs in the same batch. (c) The example of PCR. It only calculates similarities of selective anchor-to-proxy pairs in the same batch. (d) The example of contrastive component. It produces anchor-to-sample pairs to PCR. (e) The illustration of the temperature component. It decouples the temperature coefficient into two parts based on their impacts on gradients and sets them in different ways. (f) The illustration of the distillation component. PCD distills old anchor-to-proxy pairs to the new ones, and SCD constrains new anchor-to-sample pairs using the old ones.

edge of anchor-to-sample relations for the samples in a training batch, where the model can obtain more abundant semantic information. The selection of anchor-to-sample pairs can provide a novel way of pair selection for the proxy-based replay manner. Since previous studies [11], [12] have proved that suitably selecting anchor-to-proxy pairs is effective in addressing the “bias” issue. Hence, the contrastive-based replay manner can provide informative anchor-to-proxy pairs for the proxy-based replay manner. Therefore, it is beneficial to develop a coupling manner to keep these advantages at the same time.

With these inspirations, we propose a novel OCL method called proxy-based contrastive replay (PCR) [13] to alleviate the phenomenon of CF. The core motivation is the coupling of proxy-based and contrastive-based loss, and the key operation is to replace anchor-to-sample pairs with anchor-to-proxy pairs in the contrastive-based loss. As shown in Figure 1(c), PCR calculates similarities between each anchor and other proxies, which is similar to the proxy-based loss. However, it only takes the proxies whose associated classes of samples appear in the same batch, which is analogous to the contrastive-based loss. And the selection way of anchor-to-proxy pairs is better than existing solutions [11], [12].

Based on PCR, we further develop a more comprehensive method named holistic proxy-based contrastive replay (HPCR), which additionally consists of three components. 1) The **contrastive component** conditionally incorporates anchor-to-sample pairs to PCR to improve the model’s ability of feature extraction, making PCR learn more fine-grained semantic information when the training batch is large. As demonstrated in Figure 1(d), we set a step function $s(N)$ to control the importance of the anchor-to-sample pairs. When the number of samples is small, their importance is 0, since these pairs would harm the performance; otherwise, it is 1. 2) The **temperature component** decouples the temperature coefficient into two parts based on their

impacts on gradients, as demonstrated in Figure 1 (e). One of the two parts is set as a static constant value and the other is denoted as a dynamic function value to train the model, making it learn more novel knowledge. 3) Meanwhile, the **distillation component** provides more constraints for the replaying process of previous samples to preserve more historical knowledge. As stated in Figure 1 (f), the distillation component consists of two parts: proxy-based contrastive distillation (PCD) and sample-based contrastive distillation (SCD). The former distills the old anchor-to-proxy correlations to the new ones, while the latter constrains the new anchor-to-sample correlations using the old ones.

Our main contributions can be summarized as follows:

- 1) We theoretically analyze the characteristics of proxy-based and contrastive-based replay manner, discovering their coupling manner is beneficial. To the best of our knowledge, this work is the first to combine these two manners for the OCL problem.
- 2) We propose a novel OCL framework called PCR to achieve the complementary advantages of two existing approaches. By replacing the samples for anchor with proxies in contrastive-based loss, PCR can mitigate the forgetting issue effectively.
- 3) We further develop a more holistic method based on PCR, named HPCR, which consists of a contrastive component, a temperature component, and a distillation component. These three components improve the model’s feature extraction ability, generalization ability, and anti-forgetting ability, respectively.
- 4) We conduct extensive experiments on four datasets, and the empirical results consistently demonstrate the superiority of HPCR over various state-of-the-art methods. We also investigate and analyze the benefits of each component by ablation studies. And the codes are open-sourced at <https://github.com/FelixHuiweiLin/PCR>.

This work is an extension to our conference version in [13]. This work is more holistic and can be divided into the following four aspects. (i) This version provides a gradient analysis of PCR, improving its theoretical rationality. (ii) This version conditionally incorporates anchor-to-sample pairs to PCR and takes it as a contrastive component, enhancing the model's ability of feature extraction. (iii) This version additionally proposes a temperature component to improve the model's generalization capability, and a distillation component to enhance the model's anti-forgetting capability. (iv) More experiments are conducted to explore the proposed method, including a new dataset (Split Tiny-ImageNet), more ablation studies, and visualization.

2 RELATED WORK

2.1 Continual Learning

Since continual learning generally exists in various scenarios [14], [15], [16], [17] of deep learning, its related researches are quite extensive. In addition to the work related to the innovation and application of continual learning methods, the analysis [18], [19] and overview [2], [6] work also have attracted much attention.

The Setups of Continual Learning. There are many continual learning setups that have been discussed recently [20]. 1) First, continual learning can be divided into task-based continual learning (multi-head setup) and task-free continual learning (single-head setup) by whether the task-ID is given in the testing process. Task-based continual learning [5] assumes that task-ID can be available while the network in task-free continual learning [21], [22], [23] has no access to task-ID at inference time. 2) Next, depending on how to train the network, we can categorize continual learning into offline learning setup and online learning setup. Under the offline learning setting [24], all training samples in the current learning stage are not only allowed to be accessed by the network but also learned with multiple training steps. In contrast, each training sample in the streamed data is seen only once for the online learning setup [6]. 3) Finally, following [25], continual learning also can be separated into disjoint-task and blurry-task setups. The disjoint-task setup requires that the intersection of the label sets of any two learning stages is an empty set [26]. The blurry-task setup has been proposed to set some common samples for the training samples of each learning stage [27].

The Methods of Continual Learning. Recent advances in continual learning are driven by three main directions. 1) **Architecture-based methods**, also known as parameter-isolation methods, divide each task into a set of specific parameters of the model. They dynamically extend the model as the task increases [28] or gradually freeze part of parameters to overcome the forgetting problem [29]. 2) **Regularization-based methods**, also called prior-based methods, store the historical information learned from old data as the prior knowledge of the network. It consolidates past knowledge by extending the loss function with an additional regularization term. Some approaches [30] estimate the importance of each network parameter to the old classes and selectively penalize its changes. The others [31] exploit knowledge distillation [32] among the consecutive tasks, appointing a past version of the model as a teacher

to constrain the learning stage of new data. 3) **Replay-based methods**, which set a fixed-size memory buffer or generative model to store, produce, and replay historical samples in the future training process, also goes by the name of rehearsal-based methods. On the one hand, some of them are effective in generating synthesized samples using a generator that is trained along with the learner [33], [34], [35], [36]. However, this kind of method tends to synthesize unknown samples that do not belong to any class setting on complex datasets, hurting the performance of the model. On the other hand, others that replay old data with new data are still the most effective for knowledge anti-forgetting at present [37]. A large number of approaches [38], [39], [40], [41], [42] have been proposed to improve the performance of replaying. Instead of replaying, some approaches [43], [44], [45], [46] focus on the optimization process.

In this work, the setup is online continual learning based on the disjoint-task setup with a task-free process. Compared with general continuous learning, this setup is more practical and difficult. In such a scenario, HPCR is proposed as a novel replay-based method to address the forgetting issue. Different from general replay-based methods, HPCR is used to quickly learn novel knowledge and efficiently retain historical knowledge in an online fashion.

2.2 Online Continual Learning

OCL is a subfield of continual learning that focuses on efficiently learning from a single pass over the online data stream, where tasks or information arrive incrementally over time. It is essential in scenarios where a model needs to continuously evolve its knowledge and adapt to new information [6]. Researchers in this field focus on developing algorithms and techniques to mitigate catastrophic forgetting, control model adaptation, and efficiently use limited resources to achieve this continuous learning. At present, the replay-based methods are the main solutions of OCL. Only AOP [47], which is based on orthogonal projection, has been proposed for OCL without replaying. Although architecture-based methods can be effective for continual learning, they are often impractical for OCL. Since it is unfeasible for large numbers of tasks [48] by the "incremental network architectures". Meanwhile, it is known that regularization-based methods show poor performance in OCL as it is hard to design a reasonable metric to measure the importance of parameters [48].

Experience replay (ER) [49] that employs reservoir sampling for memory management is usually a strong strategy. Many subsequent methods have been improved based on this method and can generally be divided into three groups. 1) Some approaches belong to **memory retrieval strategy**, which usually studies how to select more important samples from the buffer for replaying. These representative methods include MIR [50] using increases in loss, and ASER [51] using adversarial shapley value. 2) In the meantime, some approaches [52], [53], [54], [55] focus on saving more effective samples to the memory buffer, belonging to the **memory update strategy**. The core of this type of method is to use the limited samples in the buffer to approximate all previous samples as much as possible. 3) In addition to selecting important samples, it is equally important to

conduct efficient anti-forgetting training. The **model update strategy** is a family of methods [7], [12], [56], [57], [58], [59], [60], [61], [62] to improve the learning efficiency, making the model learn quickly and memory efficiently. All of them belong to the proxy-based replay manners except SCR [56], which uses a contrastive-based replay manner.

The proposed HPCR in this work is a novel model update strategy for OCL. Different from existing approaches that use only one manner, it aims to combine the contrastive-based replay manner with the proxy-based replay manner. By complementing their advantages, the coupling manner can more effectively address the forgetting issue. Besides, HPCR decouples the original temperature into two parts based on their impacts on gradients and sets them in different ways, which are different methods. Finally, the proposed contrastive component distillates the correlations of anchor-to-proxy and anchor-to-sample in the meantime, which can be more suitable for HPCR than existing studies.

2.3 Deep Metric Learning

Similar to [9], our method is inspired by deep metric learning, trying to exploit the strengths of representations. Deep metric learning aims to measure the similarity among samples by a deep neural network while using an optimal distance metric for learning tasks [63]. Generally, the loss functions for this learning task can be categorized into pair-based and proxy-based losses. For one thing, the pair-based methods [64], [65], [66], [67] can mine rich semantic information from anchor-to-sample relations, but converge slowly due to its high training complexity. Since contrastive-based loss is good at learning anchor-to-sample pairs, it can be regarded as a type of pair-based method. For another thing, the proxy-based methods [68], [69] converge fast and stably, meanwhile may miss partial semantic information by learning anchor-to-proxy relations. Their loss functions consist of an anchor sample with similar and dissimilar learned proxies. The cross-entropy loss can be regarded as a type of proxy-based method.

The proposed HPCR in this work integrates these two types of methods. Different from existing studies, HPCR is proposed to quickly learn novel knowledge and effectively keep historical knowledge for OCL.

3 PROBLEM STATEMENT AND ANALYSIS

3.1 Problem Formulation

In the problem of classification, OCL divides a data stream into a sequence of learning tasks as $\mathcal{D} = \{\mathcal{D}_t\}_{t=1}^T$, where $\mathcal{D}_t = \{\mathcal{X}_t \times \mathcal{Y}_t, \mathcal{C}_t\}$ contains the samples \mathcal{X}_t , corresponding labels \mathcal{Y}_t , and task-specific classes \mathcal{C}_t . Different tasks have no overlap in the classes. All of learned classes are denoted as $\mathcal{C}_{1:t} = \bigcup_{k=1}^t \mathcal{C}_k$. The neural network is made up of a feature extractor $\mathbf{z} = h(\mathbf{x}; \Phi)$ and a softmax (proxy-based) classifier $\mathbf{o} = f(\mathbf{z}; \mathbf{W}) = [\mathbf{o}_c]_{c \in \mathcal{C}_{1:t}}^{\mathcal{C}_{1:t}}$ [70], where $\mathbf{o}_c = \langle \mathbf{z}, \mathbf{w}_c \rangle / \tau$ is the i th dimension value of \mathbf{o} , $\langle \cdot, \cdot \rangle$ is the cosine similarity, γ is a scale factor and $\mathbf{W} = [\mathbf{w}_1, \mathbf{w}_2, \dots, \mathbf{w}_c]$ contains trainable proxies of all classes. The categorical probability that sample \mathbf{x} belongs to class y is

$$p_y = \frac{\exp(o_y)}{\sum_{c \in \mathcal{C}_{1:t}} \exp(o_c)}. \quad (1)$$

In the training process, the model can only access \mathcal{D}_t and each sample can be seen only once. Specifically, it learns each mini-batch current samples $\mathcal{B} \subset \mathcal{D}_t$ by

$$L = E_{(\mathbf{x}, y) \sim \mathcal{B}} [-\log(p_y)]. \quad (2)$$

Such a training strategy is known as **Finetune**, where the model learns without any anti-forgetting operations. In the inference process, the model predicts each unknown instance by a softmax classifier

$$y^* = \arg \max_c p_c, c \in \mathcal{C}_{1:t}. \quad (3)$$

3.2 Analysis of Catastrophic Forgetting.

A direct cause of CF is the unbalanced gradient propagation between old and new classes. The gradient for a single sample $\{\mathbf{x}, y\}$ can be expressed as

$$\frac{\partial L}{\partial \langle \mathbf{z}, \mathbf{w}_c \rangle} = \begin{cases} (p_y - 1)/\tau, & c = y \\ (p_c)/\tau, & c \neq y \end{cases}. \quad (4)$$

As Equation (4) shows, if a training sample \mathbf{x} belongs to class y , it not only increases the logits value of the y -th dimension by $p_y - 1 < 0$, but also decreases the logits value of other dimension by $p_c > 0$. Combining with the chain rule, it provides the positive gradient for the proxy of class y as $\langle \mathbf{z}, \mathbf{w}_y \rangle = \langle \mathbf{z}, \mathbf{w}_y \rangle - \eta(p_y - 1)/\tau$, and propagates the negative gradient to the other proxies as $\langle \mathbf{z}, \mathbf{w}_c \rangle = \langle \mathbf{z}, \mathbf{w}_c \rangle - \eta(p_c)/\tau$. Since η is a positive learning rate and τ is also a positive temperature scale. Furthermore, the gradient is transferred to the feature extractor, making it focus on the features that can distinguish this class from other classes.

When directly optimizing Equation (2), the learning of new classes dominates the gradient propagation, causing the phenomenon of CF. To better analyze it, we show a case that learns the samples of the cat and dog at the first task (Figure 2(a)) and then learns the samples of ship and airplane at the next task (Figure 2(b)-(f)). As seen in the left part of Figure 2(b), the gradient is produced by learning new classes. As a result, the proxies of new classes receive more positive gradients (\uparrow) and the others obtain more negative gradients (\downarrow). Shown as the red arrows in the left part of Figure 2(b), it causes the proxies of new classes to be close to the samples of new classes, while the proxies of old classes are far away from them. Meanwhile, the feature extractor pays more attention to the features of new classes. It causes the samples of new and old classes to be close [12] in the unit embedding space. Hence, it is easy to classify samples into new classes.

3.3 Analysis of Proxy-based Replay Manner

ER [49] allocates a memory buffer \mathcal{M} to temporarily store part of previous samples of old classes, which are retrained with current samples. Thus, it selects a mini-batch of previous samples $\mathcal{B}_{\mathcal{M}} \subset \mathcal{M}$ to train with the current samples in \mathcal{B} . The objective function is changed to

$$L_{ER} = E_{(\mathbf{x}, y) \sim \mathcal{B} \cup \mathcal{B}_{\mathcal{M}}} [-\log(\frac{\exp(o_y)}{\sum_{c \in \mathcal{C}_{1:t}} \exp(o_c)})], \quad (5)$$

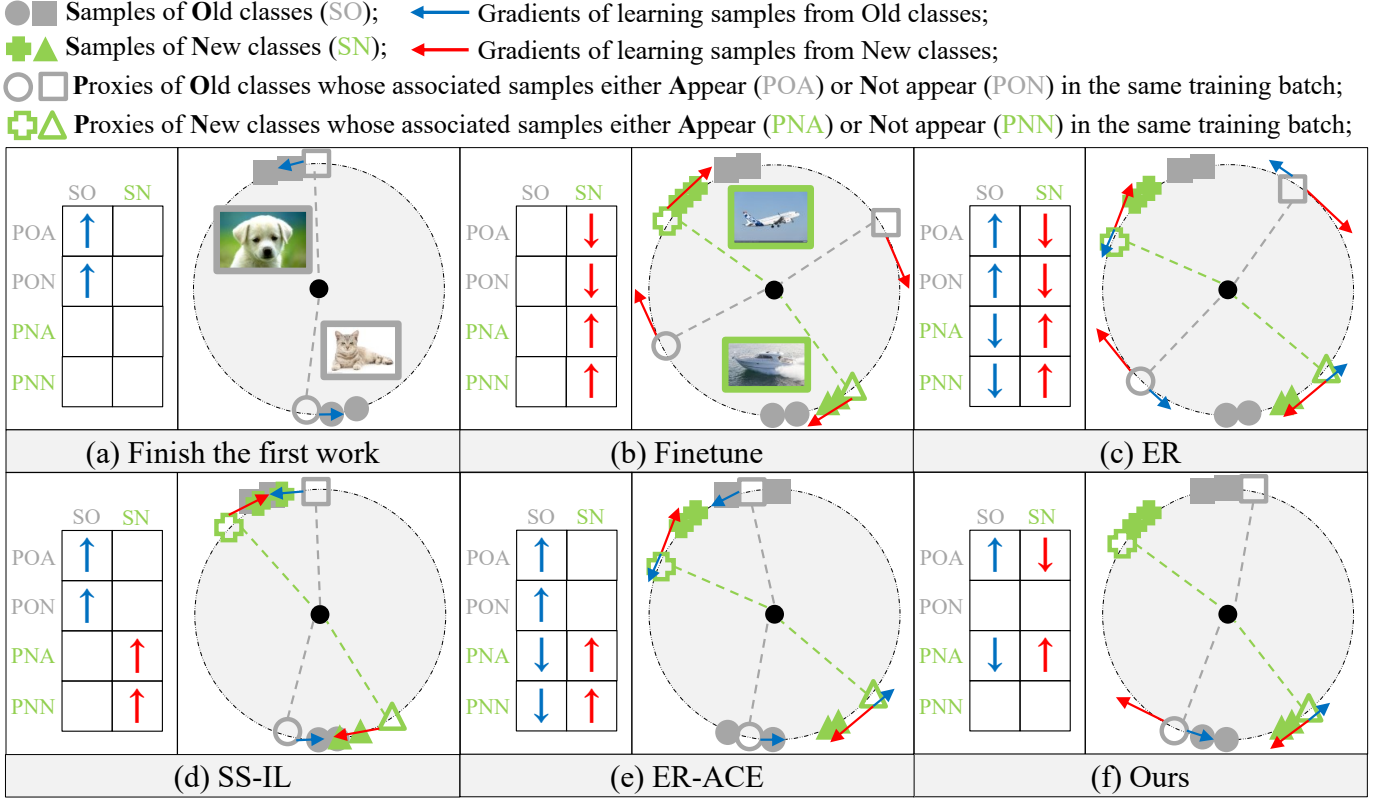


Fig. 2. Analysis of different proxy-based manners. In each sub-figure, the left part is the process of gradient propagation from samples to all proxies, and the right part is the unit embedding space of samples and proxies. (a) The learning of the first task. The gradient propagation only exists in the current two classes, denoted as the blue arrows. (b) The learning of the second task by Finetune. The new classes dominate the gradient propagation, denoted as the red arrows. (c) The learning of the second task by ER. (d) The learning of the second task by separated softmax in SS-IL. (e) The learning of the second task by ER-ACE. (f) The learning of the second task by our method. Different from existing studies, our method controls the process of gradient propagation more effectively, improving the recognition of new and old classes.

where the samples of all classes take the same way to calculate categorical probability. As described in Figure 2(c), previous samples of old classes acquire some advantages in the propagation of gradient. Not only do the proxies of old classes obtain some additional positive gradient, but also the proxies of new classes receive a negative gradient to push them away from the proxies of old classes. Although the phenomenon of CF can be alleviated to some extent, its effect is still limited. Since the number of samples for each class in the fixed buffer will decrease as the learning process goes on, the gradient of old classes is not sufficient.

SS-IL [11] separately calculates the categorical probability for old and new classes by a separated softmax as

$$\begin{aligned}
 L_{SS} = & E_{(x,y) \sim \mathcal{B}} [-\log(\frac{\exp(o_y)}{\sum_{c \in \mathcal{C}_t} \exp(o_c)})] \\
 & + E_{(x,y) \sim \mathcal{B}_{\mathcal{M}}} [-\log(\frac{\exp(o_y)}{\sum_{c \in \mathcal{C}_{1:t-1}} \exp(o_c)})].
 \end{aligned} \quad (6)$$

As demonstrated in Figure 2(d), it cuts off the propagation from the learning of old classes to the proxies of new classes and prevents the propagation from the learning of new classes to the proxies of old classes. It is able to avoid that the gradient of new classes affects the proxies of old classes. However, the model can not well distinguish new classes from old classes, since the lack of gradient makes it difficult for the model to classify samples across tasks.

ER-ACE [12] is also proposed to address the same issue by an asymmetric cross-entropy loss, which is expressed as

$$\begin{aligned}
 L_{ACE} = & E_{(x,y) \sim \mathcal{B}} [-\log(\frac{\exp(o_y)}{\sum_{c \in \mathcal{C}_t} \exp(o_c)})] \\
 & + E_{(x,y) \sim \mathcal{B}_{\mathcal{M}}} [-\log(\frac{\exp(o_y)}{\sum_{c \in \mathcal{C}_{1:t}} \exp(o_c)})].
 \end{aligned} \quad (7)$$

Its categorical probability of new classes is similar to SS-IL, and the categorical probability of old classes is the same as ER. In detail, it only selects part of anchor-to-proxy pairs for the learning of new classes. As shown in Figure 2(e), it only breaks the gradient propagation from the learning of new classes to the proxies of old classes. Keeping the gradient from the learning of old classes to the proxies of new classes helps to avoid the inseparable situation of SS-IL. Although it is beneficial for old classes, the performance of new classes is harmed.

3.4 Analysis of Contrastive-based Replay Manner

SCR [56] is proposed as a good alternative for OCL by contrastive-based loss, which is denoted as

$$\begin{aligned}
 L_{SCR} = & E_{(x,y) \sim \mathcal{B} \cup \mathcal{B}_{\mathcal{M}}} \\
 & [-\frac{1}{|\mathcal{P}|} \sum_{p \in \mathcal{P}} \log \frac{\exp(\langle z, z_p \rangle / \tau)}{\sum_{j \in \mathcal{J}} \exp(\langle z, z_j \rangle / \tau)}].
 \end{aligned} \quad (8)$$

It splices current samples and previous samples into the same batch and calculates the similarities of anchor-to-sample pairs. \mathcal{J} is the indices set of samples except for anchor x in the same batch, while \mathcal{P} denotes the set of samples with the same labels as anchor x . Different from proxy-based loss, the selected pairs do not rely on the number of classes but are related to the number of samples in a training batch. At the same time, it abandons the softmax classifier with bias issues and inferences by an NCM classifier

$$y^* = \arg \min_c \|\mathbf{z} - \boldsymbol{\mu}_c\|, c \in C_{1:t}. \quad (9)$$

To obtain the classification centers $\boldsymbol{\mu}_c$ of all classes, the NCM classifier has to compute the embeddings of all samples in the memory buffer before each inferring. Hence, its effect is constrained by the size of the memory buffer and batch size. And its performance would be not satisfactory when less samples to replay.

3.5 Motivation

Why not couple these two replay manners to achieve complementary advantages? From the above analysis, we can draw three conclusions about OCL.

First and foremost, the unbalanced gradient propagation between new classes and old classes is the main cause of CF for replay-based methods. The new classes dominate this process, making the samples of new classes highly distinguishable but the ones of old classes indivisible. Effectively controlling the gradient propagation between old and new classes can help the model alleviate the forgetting problem.

Besides, proxy-based replay manners are commonly used and effective for OCL. It tries to explore the relations of samples from all anchor-to-proxy pairs through cross-entropy loss. By softmax classifier, it straightly classifies a testing sample by proxies and it is also applicable when the samples are few. Although some fine-grained semantic information will be lost, this type of method is stable and efficient with fast convergence since its training complexity is low. The main problem of it is the “bias” issue. Existing approaches control the gradient propagation by selecting part of anchor-to-proxy pairs to calculate the objective function. Although they are effective, they are easy to hurt the generalization ability of the model to learn new classes.

Last but not least, contrastive-based replay manners are proposed to avoid the biased phenomenon. It aims to learn reliable representations for all samples by anchor-to-sample pairs. Its contrastive-based loss depends on the samples from the same batch, which is different from the proxy-based one supported by all proxies. It addresses the bias problem by replacing the softmax classifier with the NCM classifier, which uses the samples in the buffer to calculate classification centers for all classes. With the help of various anchor-to-sample pairs, it can obtain more fine-grained semantic knowledge. However, its effectiveness depends on a large batch of training data and a large capacity of the buffer. Moreover, due to the high complexity of training, the effect is unstable and the speed of convergence is slow. Some similar studies have been proposed to use proxy to mitigate the problem of contrastive-based loss [9], [71].

Based on these conclusions, the inspiration is to couple two replay manners and achieve complementary advantages. The characteristics of these two replay manners

are summarized in Table 1. For one thing, the anchor-to-proxy pairs of proxy-based replay manner can overcome the disadvantage of contrastive-based loss. For another thing, the selection of anchor-to-sample pairs in contrastive-based loss provides a heuristic way to select anchor-to-proxy pairs for proxy-based replay manner. Moreover, the anchor-to-sample pairs contain richer fine-grained semantic knowledge than the anchor-to-proxy pairs. Hence, the coupling of these two manners would lead to a better solution.

How to couple these two replay manners? The most intuitive way is to add two different loss functions as

$$L_{couple}^1 = L_{SCR} + L_{ER}. \quad (10)$$

It aims to mine the anchor-to-sample and anchor-to-proxy relations in the meantime. It has been applied to research on data imbalance tasks [71]. In offline learning, these works usually use contrastive-based loss to learn the feature extractor of the model, and then use a balanced sub-dataset to learn the softmax classifier. However, the two-stage learning way is not suitable for OCL due to timeliness requirements. Therefore, these two steps should be simultaneously executed in an online fashion.

Another way of coupling is the loss in [9] for domain generalization. It adds anchor-to-sample pairs to cross-entropy loss as

$$L_{couple}^2 = E_{(x,y) \sim \mathcal{B} \cup \mathcal{B}_M} [-\log(\frac{\exp(o_y)}{\sum_{c \in \mathcal{C}_{1:t}} \exp(o_c) + \sum_{j \in \mathcal{J}} \exp(\langle \mathbf{z}, \mathbf{z}_j \rangle / \tau)})]. \quad (11)$$

It associates each anchor with all samples in a mini-batch of training. Meanwhile, it uses all class proxies to form the anchor-to-proxy pairs for the anchor.

Nevertheless, these ways still cannot take advantage of each replay manner to address the forgetting issue of OCL. Since they ignore that the key is to select anchor-to-proxy pairs in a contrastive way and train by these pairs. Specifically, we replace the samples of anchor-to-sample pairs with proxies in contrastive-based loss as

$$L_{ours} = E_{(x,y) \sim \mathcal{B} \cup \mathcal{B}_M} [-\frac{1}{|\mathcal{P}|} \sum_{p \in \mathcal{P}} \log \frac{\exp(o_p)}{\sum_{j \in \mathcal{J}} \exp(o_j)}]. \quad (12)$$

Different from existing studies, its way of computing categorical probability is changed for each mini-batch. On one hand, such a loss has faster convergence speed and better robustness and can cope with a small number of samples with the help of proxies. On the other hand, the replacing proxies are only from the classes that appear in the training batch. As a result, the gradient for propagation is only from the learning of these classes. As shown in Figure 2(f), the gradients among all proxies are not completely separated in the whole training process. The gradient propagation only occurs when the corresponding classes appear in the same batch. Meanwhile, in each learning step, only new and old classes in the current batch participate in the gradient propagation. The proxies of old classes, which are affected by the negative gradient of new classes, can also generate the positive gradient for confrontation and further mitigate the forgetting problem. Hence, the samples of all classes can be recognized more correctly than existing methods.

TABLE 1
The characteristics of the proxy-based and contrastive-based replay manners.

Replay Manner	Classifier	Pairs of Loss	Advantages	Disadvantages
Proxy-based	Softmax	All Anchor-to-proxy Pairs	Fast Convergence Stable	Bias Incomplete Semantic Knowledge
Contrastive-based	NCM	Selective Anchor-to-sample Pairs	Avoid Bias Complete Semantic Knowledge	Slow Convergence Unstable

Algorithm 1 Proxy-based Contrastive Replay

Input: Dataset D , Learning Rate λ , Scale factor γ
Output: Network Parameters θ
Initialize: Memory Buffer $\mathcal{M} \leftarrow \{\}$, Network Parameters $\theta = \{\Phi, W\}$

```

1: for  $t \in \{1, 2, \dots, T\}$  do
2:   // Training Procedure
3:   for mini-batch  $\mathcal{B} \subset D_t$  do
4:      $\mathcal{B}_{\mathcal{M}} \leftarrow \text{RandomRetrieval}(\mathcal{M})$ 
5:      $\mathcal{B} \cup \mathcal{B}_{\mathcal{M}} \leftarrow \text{Concat}([\mathcal{B}, \mathcal{B}_{\mathcal{M}}])$ 
6:      $L \leftarrow \text{Equation (13)}$ 
7:      $\theta \leftarrow \theta + \lambda \nabla_{\theta} L$ 
8:      $\mathcal{M} \leftarrow \text{ReservoirUpdate}(\mathcal{M}, \mathcal{B})$ 
9:   end for
10:  // Inference Procedure
11:   $m \leftarrow \text{number of testing samples}$ 
12:  for  $k \in \{1, 2, \dots, m\}$  do
13:     $y_k^* \leftarrow \arg \max_c p_c, c \in C_{1:t}$ 
14:  end for
15:  return  $\theta$ 
16: end for

```

4 PROXY-BASED CONTRASTIVE REPLAY

With these inspirations, we propose a novel proxy-based contrastive replay (PCR) framework, and the technical details will be stated in this section. The framework consists of a CNN-based backbone $z = h(x; \Phi)$ and a proxy-based classifier $f(z; W)$. The whole training and inference procedures of PCR are summarized in Algorithm 1.

4.1 The Training Procedure of PCR

In this part, the model is trained by learning samples of new classes and replaying samples of old classes. For each step, given current samples \mathcal{B} , it randomly retrieves previous samples $\mathcal{B}_{\mathcal{M}}$ from the memory buffer (lines 1-4). Besides, these samples are spliced together for the batch of training (line 5). Then, the model is optimized by this training batch (lines 6-7). The objective function is defined as

$$L_{PCR} = E_{(x,y) \sim \mathcal{B} \cup \mathcal{B}_{\mathcal{M}}} [-\log(\frac{\exp(o_y)}{\sum_{c \in C_{1:t}} k_c \exp(o_c)})]. \quad (13)$$

where k_c is the number of samples belonging to class c in the training batch. If $k_c = 0$, the proxy of class c does not participate in the gradient propagation, as its samples do not appear in the current training step. Finally, it updates the memory buffer by reservoir sampling strategy (line 8), which can ensure that the probability of each sample being extracted is equal. Conveniently, the memory buffer in our framework has a fixed size, no matter how large the amount of samples is.

4.2 The Inference Procedure of PCR

The inference procedure (lines 11-15) is different from the training procedure. Each testing sample x_k obtains its class probability distribution by Equation (1). And we perform the inference prediction to x_k with highest probability as

$$y_k^* = \arg \max_c p_c, y \in C_{1:t}. \quad (14)$$

4.3 The Gradient Analysis of PCR

In PCR, the categorical probability that the sample x belongs to class c is

$$p_y^* = \frac{\exp(o_y)}{\sum_{c \in C_{1:t}} k_c \exp(o_c)}. \quad (15)$$

Similar to conventional proxy-based loss, we can also calculate the gradient of PCR for a single sample x as Theorem 1.

Theorem 1. In PCR, the gradient for all proxies is

$$\frac{\partial L_{PCR}}{\partial \langle z, w_c \rangle} = \begin{cases} (k_y p_y^* - 1)/\tau, & c = y \\ (k_c p_c^*)/\tau, & c \neq y \end{cases}. \quad (16)$$

Proof: By chain-rule, we have

$$\frac{\partial L_{PCR}}{\partial \langle z, w_c \rangle} = \left(\frac{\partial L}{\partial p_c^*} \frac{\partial p_c^*}{\partial f(z; W)} \right) \frac{\partial f(z; W)}{\partial \langle z, w_c \rangle}. \quad (17)$$

If $c = y$, we can get

$$\begin{aligned} & \frac{\partial L_{PCR}}{\partial p_c^*} \frac{\partial p_c^*}{\partial f(z; W)} \\ &= \frac{-1 \exp(o_y) (\sum_{c \in C_{1:t}} \exp(o_c) - k_y \exp(o_y))}{p_y^* (\sum_{c \in C_{1:t}} k_c \exp(o_c))^2} \\ &= \frac{-1}{p_y^*} (p_y^* - k_y p_y^* p_y^*) = k_y p_y^* - 1. \end{aligned} \quad (18)$$

Otherwise, if $c \neq y$, we can get

$$\begin{aligned} & \frac{\partial L_{PCR}}{\partial p_c^*} \frac{\partial p_c^*}{\partial f(z; W)} \\ &= \frac{-\exp(o_c) - k_c \exp(o_c) \exp(o_y)}{p_c^* \exp(o_y) (\sum_{c \in C_{1:t}} k_c \exp(o_c))^2} \\ &= \frac{-1}{p_c^*} (-k_c p_c^* p_c^*) = k_c p_c^*. \end{aligned} \quad (19)$$

Since $\partial f(z; W) / \partial \langle z, w_c \rangle = 1/\tau$, the final gradient can be denoted as Equation (16).

The gradient in Equation (16) is different from the one in Equation (4). For one thing, the gradient only influences the proxies whose associated samples exist in the same training batch. For example, when learning a current sample x_y belongs to class y , the gradient for the proxy of class c is $(k_c p_c^*)/\tau$ if x_c is in the same batch; otherwise it is none

since $k_c = 0$ if \mathbf{x}_c is not selected. Due to only retaining partial proxies, the gradient propagation efficiency of these selected proxies will be greatly improved. For another thing, the gradient can be affected by the number of samples in a training batch. For instance, if there are two current samples belonging to class y in a training batch, the values of $k_y p_y^* - 1$ and $k_y p_y^*$ tend to be smaller than the ones with a current sample. It can constrain the positive gradient for the proxy of class y as well as the negative gradient for the proxy of other classes. At the same time, if there is only one previous sample \mathbf{x}_c , which is less than the number of current samples. Its positive gradient for the class c can be increased while the negative gradient for the class y can be decreased.

5 HOLISTIC PROXY-BASED CONTRASTIVE REPLAY

With the help of PCR, the model alleviates the phenomenon of catastrophic forgetting by selecting some proxies instead of all proxies to learn current samples and replay previous samples. In such a learning way, the old classes whose associated proxies are not selected can avoid the bias caused by unbalanced gradient competition. However, PCR is still not the optimal solution as it has a few limitations that have not been addressed. 1) PCR only considers the relations of anchor-to-proxy but ignores the relations of anchor-to-sample, which leads to the model losing some important semantic information. The anchor-to-sample pairs can improve the model's ability of feature extraction in a large training batch, which is crucial for PCR. 2) The setting of temperature coefficient τ in PCR is too simplistic. Due to the fact that the temperature coefficient also affects the gradient propagation process of PCR, simply using a static constant is not the best choice. 3) Those old classes that have been selected to learn together with new classes still face the issue of bias in the training process. To address these problems, we develop holistic proxy-based contrastive replay (HPCR), an improved PCR-based method consisting of three components.

5.1 Contrastive Component of HPCR

The contrastive component conditionally incorporates the anchor-to-sample pairs to PCR and improves the model's ability of feature extraction. The anchor-to-sample pairs contain richer fine-grained semantic information compared to anchor-to-proxy pairs. Although extracting the relations of anchor-to-sample is easily limited by the number of samples in a training batch, it can still play a crucial role when the batch size is sufficient. Hence, the contrastive component of HPCR is denoted as

$$L_{PCR_C} = E_{(\mathbf{x}, y) \sim \mathcal{B} \cup \mathcal{B}_M} \left[\frac{-1}{|\mathcal{P}|} \sum_{p \in \mathcal{P}} \log \left(\frac{\exp(o_y) + s(N) \cdot \exp(\langle \mathbf{z}, \mathbf{z}_p \rangle / \tau)}{\sum_{c \in \mathcal{C}_{1:t}} k_c \exp(o_c) + \sum_{j \in \mathcal{J}} s(N) \cdot \exp(\langle \mathbf{z}, \mathbf{z}_j \rangle / \tau)} \right) \right]. \quad (20)$$

Here, $s(N)$ is a self-defined step function used to control the importance of anchor-to-sample pairs, and it is defined as

$$s(N) = \begin{cases} 0, & N < N_{min} \\ 1, & N \geq N_{min} \end{cases}. \quad (21)$$

N is the number of samples in the current training batch, and N_{min} is a hyper-parameter used to determine whether to use anchor-to-sample pairs. When the size of the training batch is small, the correlation between samples is prone to noise affecting the performance of the model. Therefore, their importance should be set to 0. At this point, PCR_C degenerates into PCR; otherwise, the importance of these samples should be set to 1 to improve the model's feature extraction ability. Compared to the PCR, PCR_C can not only mine the relations of anchor-to-proxy, but also explore the relations of anchor-to-sample. It increases inter-class distance as well as decreases intra-class distance.

5.2 Temperature Component of HPCR

5.2.1 The Analysis of Temperature Coefficient

In Equation (16), the propagation process of gradients is influenced by an important factor τ , which is called the temperature coefficient. In a proxy-based classifier, the norm of vectors has been proved to be unfriendly to continual learning and thus abandoned [70]. However, the retained similarity of vectors $\langle \mathbf{z}, \mathbf{w} \rangle$ has a value range of $[-1, 1]$, which brings certain difficulties to the optimization of the model. Hence, τ in p_c^* is used to control the strength of $\langle \mathbf{z}, \mathbf{w} \rangle$, which is vital to find the optimal solution.

Inspired by [72], we define a relative penalty $r(\langle \mathbf{z}, \mathbf{w}_c \rangle)$ on negative proxy $\mathbf{w}_c (c \neq y)$ for the sample (\mathbf{x}, y) by

$$r(\langle \mathbf{z}, \mathbf{w}_c \rangle) = \frac{\left| \frac{\partial L}{\partial \langle \mathbf{z}, \mathbf{w}_c \rangle} \right|}{\left| \frac{\partial L}{\partial \langle \mathbf{z}, \mathbf{w}_y \rangle} \right|} = \frac{k_c \exp(o_c)}{\sum_{j \neq y} k_j \exp(o_j)}, c \neq y. \quad (22)$$

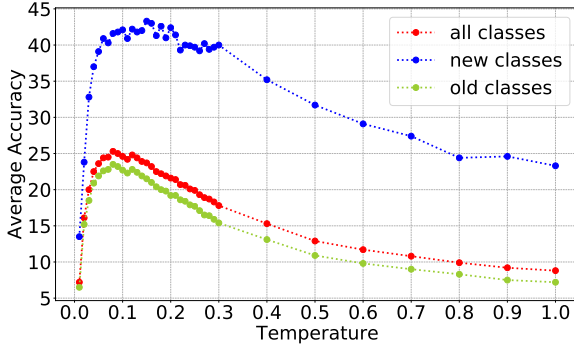
It can reflect the strength of penalties on all negative samples. As τ increases, the distribution of $r(\langle \mathbf{z}, \mathbf{w}_c \rangle)$ is relatively uniform, and the model tends to treat all negative proxies with the same strength. On the contrary, the model pays more attention to the negative proxies with higher similarities when τ decreases.

Furthermore, small τ is more suitable for replaying old classes, while large τ is more suitable for learning new classes in OCL. Generally, the number of samples in old classes is small while the number of samples in new classes is large in OCL. This leads to the samples of old classes being more likely to become negative samples with shorter distances, while the samples of old classes tend to become negative samples with larger distances. As a result, large τ will prompt the model to pay more attention to the samples of new classes with larger distances, making it easy to ignore samples from old classes. In contrast, small τ will urge the model to focus on the samples of old classes with shorter distances, resulting in the information loss from new classes.

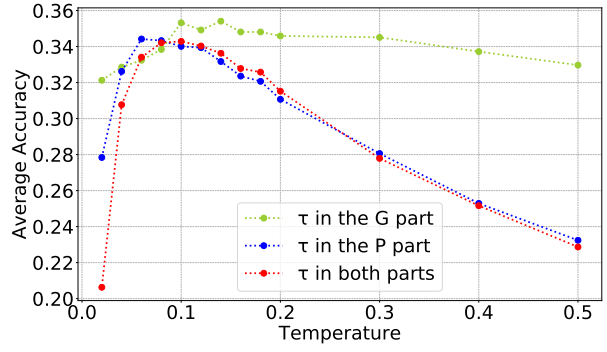
Finally, as seen in Equation (16), τ affects the process in two parts. For one thing, it directly changes the value of the gradient by $1/\tau$ (denoted as G part). For another thing, it smooths the probability distribution p_c^* of samples to implicitly adjust the gradient ((denoted as P part). Moreover, the P part has a more complex impact than the G part due to its stronger non-linearity.

5.2.2 The Influence of Temperature Coefficient

The performance of PCR would be highly sensitive to τ . To validate this viewpoint, we conduct experiments for PCR



(a) The performance on different classes



(b) The performance on different parts

Fig. 3. The performance of PCR on Split CIFAR100 (buffer size=1000) with different value of τ .

TABLE 2
The best τ for each class on Split CIFAR10 (buffer size=100).

class	0	1	2	3	4	5	6	7	8	9
type	old	old	old	old	old	old	old	old	new	new
τ	0.01	0.14	0.16	0.17	0.12	0.20	0.06	0.09	0.14	0.2

with different values of τ , and the results are shown in Figure 3. In addition to the final accuracy rate of all classes, we also report the ones of new and old classes separately. In Figure 3(a), we can make the following observations: 1) The performances of all, old, and new classes are sensitive to τ . For example, when τ changes from 0.01 to 0.2, the performance of PCR in all aspects would first increase and then decrease. 2) The sensitivity of old and new classes w.r.t. τ is different, and their best τ are different from each other. The performance on new classes reaches the best result when $\tau \in [0.1, 0.2]$ while the performance on old classes reaches the best result when $\tau \in [0.0, 0.1]$.

At the same time, we also demonstrate the performance when different τ are taken in different parts. In Figure 3(b), the lines of green, blue, and red denote the performance when τ changes in the G part, the P part, and both parts. For the G part, we keep $\tau = 0.09$ for p_c^* and only change the value of τ for $1/\tau$. On the contrary, τ is set as 0.09 for $1/\tau$ and changed from 0.0 to 0.5 in the P part. Comparing the results of the two cases, we find that the performance of the model is more sensitive to changes in τ in the G part. Meanwhile, the model exhibits greater fluctuations when τ reaches the optimal value in the P part. Although the performance of the P part appears stable with changes in τ , the accuracy of each class actually changes. Conveniently, we report the best τ for each class on Split CIFAR10 in the P part when the buffer size is 100. As stated in Table 2, to achieve the highest accuracy, the value of τ for each class is different. In a word, the setting of τ in the P part is sensitive, which means that a static value is more suitable for it. While a dynamic value is more suitable for the G part since it allows the model to consider different classes. Therefore, the setting of τ for these two parts should be decoupled.

5.2.3 Decoupled Temperature Coefficient

To this end, we set different values of τ for the P and G parts separately. For one thing, since the performance of the model is more sensitive to the P part, we set it to a static constant value. Meanwhile, we obtain a moderate value to balance the model's attention to new and old classes

using the grid search method. For another thing, due to the different optimal τ for each class, we set a dynamic one for the G part. However, it is highly difficult to find an optimal τ for each class at any time, since the real-time requirement of OCL is really high. In such a situation, the dynamic temperature is set as a robust function independent of the class, and the function is denoted as

$$\tau(s) = (\tau_{max} - \tau_{min}) \times (1 + \cos(2\pi s/S))/2 + \tau_{min}, \quad (23)$$

where s is the current step, S is the cycle length, τ_{max} is the upper bound, and τ_{min} is the lower bound. With such a periodic dynamic function, the model can select a wide range of different temperature values during the OCL process. It helps to improve the accuracy of each class and thus enhance the overall generalization ability of the model. With this temperature component, the Equation (20) can be improved to

$$L_{PCR_{CT}} = E_{(\mathbf{x}, y) \sim \mathcal{B} \cup \mathcal{B}_{\mathcal{M}}} \left[\frac{-1}{|\mathcal{P}|} \sum_{p \in \mathcal{P}} \frac{\tau}{\tau(t)} \log \left(\frac{\exp(o_y) + s(N) \cdot \exp(\langle \mathbf{z}, \mathbf{z}_p \rangle / \tau)}{\sum_{c \in \mathcal{C}_{1:t}} k_c \exp(o_c) + \sum_{j \in \mathcal{J}} s(N) \cdot \exp(\langle \mathbf{z}, \mathbf{z}_j \rangle / \tau)} \right) \right]. \quad (24)$$

Moreover, its corresponding gradient is transformed into

$$\frac{\partial L_{PCR}}{\partial \langle \mathbf{z}, \mathbf{w}_c \rangle} = \begin{cases} (k_y p_y^* - 1) / \tau(t), & c = y \\ (k_c p_c^*) / \tau(t), & c \neq y \end{cases}. \quad (25)$$

5.3 Distillation Component of HPCR

Knowledge distillation [32] has been proven to utilize historical knowledge to constrain the learning process of current samples, playing a role in mitigating the forgetting problem. As a method of knowledge distillation, DER [38] tries to retain the logits output obtained from the model during learning as historical knowledge for sample replaying. This is to improve the diversity of historical knowledge and avoid the problem of knowledge singularity caused by saving old models to store historical knowledge. However, existing DER has to use all proxies to calculate a loss function of distillation. If distilling as DER, the proxies excluded by PCR will continue to participate in gradient propagation.

To avoid this situation, we propose a novel distillation method called proxy-based contrastive distillation (PCD). Similar to PCR, the categorical probability in PCD only uses the proxies that appear in the training batch. Specifically, when saving a current sample into the memory buffer, we

not only save its instance x and label y , but also store its logits output of proxy-based classifier o^* . If the sample is selected as a previous sample to replay, its o^* can be used to keep richer historical knowledge. Hence, we can calculate the PCD loss by minimizing the Euclidean distance between the weighted logits as

$$L_{PCD} = E_{(x,y,o^*) \sim \mathcal{B}_M} \left[- \sum_c^{C_{1:t}} k_c (o_c - o_c^*)^2 \right]. \quad (26)$$

In addition to the distribution distillation of previous samples, relation distillation between samples is also necessary. Since the relation of samples not only reflects intra-class information, but also includes inter-class correlation. Hence, we propose to compute sample-based contrastive distillation (SCD) by z^* in a training batch as

$$L_{SCD} = E_{(x,y,z^*) \sim \mathcal{B}_M} \left[- \sum_{i \in \mathcal{J}} \left(\frac{\exp(\langle z, z_i \rangle / \tau)}{\sum_{j \in \mathcal{J}} \exp(\langle z, z_j \rangle / \tau)} \log \frac{\exp(\langle z^*, z_i^* \rangle / \tau)}{\sum_{j \in \mathcal{J}} \exp(\langle z^*, z_j^* \rangle / \tau)} \right) \right], \quad (27)$$

where \mathcal{J} is the indices set of samples except for anchor x in the same batch \mathcal{B}_M . With these two distillation loss functions, the model can transfer more positive gradients to the proxies of old classes and more negative gradients to the proxies of new classes. As a result, the model's ability of anti-forgetting can be improved.

5.4 Overall Procedure of HPCR

Combining these three novel components, PCR will be enhanced as HPCR. Compared to PCR, HPCR will greatly improve the model's capability of feature extraction, generalization, and anti-forgetting in the meantime. Its objective function is denoted as

$$L_{HPCR} = L_{PCR_{CT}} + \alpha L_{PCD} + \beta L_{SCD}, \quad (28)$$

where α and β are hyper-parameters of scale for PCD and SCD, respectively. Furthermore, the whole training and inference procedures of HPCR are summarized in Algorithm 2. The main differences between Algorithm 2 and Algorithm 1 lie in the training procedure. The first difference is in the memory buffer. In addition to saving the old samples and their corresponding labels, HPCR also saves the logits and feature vectors obtained during the training process of the old samples. The second one is in the loss function. The objective function of HPCR is more integrated, which is conducive to comprehensively improving the overall performance of the model.

6 PERFORMANCE EVALUATION

In this section, we evaluate the proposed framework in various OCL experiments. We discuss the overall performance of all OCL methods, analyze the ablation study of each component, and present visualization in detail.

Algorithm 2 Holistic Proxy-based Contrastive Replay

Input: Dataset D , Learning Rate λ , Scale factor γ

Output: Network Parameters θ

Initialize: Memory Buffer $\mathcal{M} \leftarrow \{\}$, Network Parameters $\theta = \{\Phi, W\}$

```

1: for  $t \in \{1, 2, \dots, T\}$  do
2:   // Training Procedure
3:   for mini-batch  $\mathcal{B} \subset D_t$  do
4:     for  $(x, y) \in \mathcal{B}$  do
5:        $z = h(x; \Phi)$ 
6:        $o = f(z; W)$ 
7:        $(x, y) \leftarrow (x, y, o, z)$ 
8:     end for
9:      $\mathcal{B}_M \leftarrow \text{RandomRetrieval}(\mathcal{M})$ 
10:     $\mathcal{B} \cup \mathcal{B}_M \leftarrow \text{Concat}([\mathcal{B}, \mathcal{B}_M])$ 
11:     $L_{PCR_{CT}} \leftarrow \text{Equation (24)}$ 
12:     $L_{PCD} \leftarrow \text{Equation (26)}$ 
13:     $L_{SCD} \leftarrow \text{Equation (27)}$ 
14:     $L \leftarrow \text{Equation (28)}$ 
15:     $\theta \leftarrow \theta + \lambda \nabla_{\theta} L$ 
16:     $\mathcal{M} \leftarrow \text{ReservoirUpdate}(\mathcal{M}, \mathcal{B})$ 
17:  end for
18:  // Inference Procedure
19:   $m \leftarrow \text{number of testing samples}$ 
20:  for  $k \in \{1, 2, \dots, m\}$  do
21:     $y_k^* \leftarrow \arg \max_c p_c, c \in C_{1:t}$ 
22:  end for
23:  return  $\theta$ 
24: end for
```

6.1 Experiment Setup

6.1.1 Datasets

We conduct experiments on four real-world image recognition datasets for evaluation. Split CIFAR10 [73] is split into 5 tasks, and each task contains 2 classes. Split CIFAR100 [73] as well as Split MiniImageNet [74] are organized into 10 tasks, and each task is made up of samples from 10 classes. Split TinyImageNet [75], which contains 200 classes, is divided into 20 tasks, and each task contains 10 classes.

6.1.2 Evaluated Baselines

To evaluate the effectiveness of PCR, we compare it with the following four methodological categories. 1) **None-replay operations** contain IID and FINE-TUNE; 2) **Memory update strategies** include ER [49], GSS [52]; 3) GMED [53]. MIR [50] and ASER [51] belong to **memory retrieval strategies**; 4) **Model update strategies** contain A-GEM [44], ER-WA [76], DER++ [38], SS-IL [11], SCR [56], ER-ACE [12], ER-DVC [58], OCM [7], OBC [59], OnPro [62], and UER [61].

6.1.3 Evaluation Metrics

We need to measure the performance of the model for OCL. We first define $a_{i,j}$ ($j \leq i$) as the accuracy evaluated on the held-out test samples of the j th task after the network has learned the training samples in the first i tasks. Similar with [51], we can further acquire the average accuracy rate

$$A_i = \frac{1}{i} \sum_{j=1}^i a_{i,j} \quad (29)$$

TABLE 3

Final Accuracy Rate (higher is better). The best scores of our methods are in boldface, and the best scores of baselines are underlined.

Datasets	Split CIFAR10 (%)			Split CIFAR100 (%)			Split MiniImageNet (%)			Split TinyImageNet (%)		
Buffer	100	200	500	1000	2000	5000	1000	2000	5000	2000	4000	10000
IID		58.1±2.5			17.3±0.8			18.2±1.1			17.3±1.7	
FINE-TUNE		17.9±0.4			5.9±0.2			4.3±0.2			4.3±0.2	
ER (NeurIPS2019)	33.8±3.2	41.7±2.8	46.0±3.5	17.6±0.9	19.7±1.6	20.9±1.2	13.4±0.9	16.5±0.9	16.2±1.7	6.1±0.5	8.5±0.7	8.9±0.6
GSS (NeurIPS2019)	23.1±3.9	28.3±4.6	36.3±4.1	16.9±1.4	19.0±1.8	20.1±1.1	13.9±1.0	14.6±1.1	15.5±0.9	/	/	/
GMED (NeurIPS2021)	32.8±4.7	43.6±5.1	52.5±3.9	18.8±0.7	21.1±1.2	23.0±1.5	15.3±1.3	18.0±0.8	19.6±1.0	7.0±0.9	10.2±0.7	11.3±1.2
MIR (NeurIPS2019)	34.8±3.3	40.3±3.3	42.6±1.7	18.1±0.7	20.3±1.6	21.6±1.7	14.8±1.1	17.2±0.8	17.2±1.2	4.9±0.6	6.3±0.6	6.4±0.7
ASER (AAAI2021)	33.7±3.7	31.6±3.4	42.1±3.0	16.1±1.1	17.7±0.7	18.9±1.0	13.8±0.9	16.1±0.9	18.1±1.1	5.3±0.3	9.6±0.8	8.1±0.8
A-GEM (ICLR2019)	17.5±1.7	17.4±2.1	17.9±0.7	5.6±0.5	5.4±0.7	4.6±1.0	4.7±1.1	5.0±2.3	4.8±0.8	/	/	/
ER-WA (CVPR2020)	36.9±2.9	42.5±3.4	48.6±2.7	21.7±1.2	23.6±0.9	24.0±1.8	17.1±0.9	18.9±1.4	18.5±1.5	9.2±0.7	11.6±1.3	11.4±1.6
DER++ (NeurIPS2020)	40.9±1.4	45.3±1.7	52.8±2.2	17.2±1.1	19.5±1.2	20.2±1.3	14.8±0.7	16.1±1.3	15.5±1.3	6.8±0.4	8.7±0.7	9.2±0.7
SS-IL (ICCV2021)	36.8±2.1	42.2±1.4	44.8±1.6	21.9±1.1	24.5±1.4	24.7±1.0	19.7±0.9	21.7±1.0	24.4±1.6	<u>13.2±0.8</u>	<u>15.2±1.0</u>	<u>18.7±0.7</u>
SCR (CVPR-W2021)	35.0±2.9	45.4±1.0	55.7±1.6	16.2±1.3	18.2±0.8	19.3±1.0	14.7±1.9	16.8±0.6	18.6±0.5	9.9±0.4	12.6±0.6	11.1±0.5
ER-DVC (CVPR2022)	36.3±2.6	45.4±1.4	50.6±2.9	19.7±0.7	22.1±0.9	24.1±0.8	15.4±0.7	17.2±0.8	19.1±0.9	7.6±0.5	9.9±0.7	10.4±0.7
OCM (ICML2022)	44.4±1.5	49.9±1.8	55.8±2.3	20.6±1.2	22.1±1.0	22.7±1.4	13.6±0.7	16.5±0.5	19.2±0.7	8.6±0.8	11.9±0.9	12.1±0.6
ER-ACE (ICLR2022)	44.3±1.5	49.7±2.4	54.9±1.4	23.1±0.8	24.8±0.9	27.0±1.2	20.3±1.3	24.8±1.1	26.2±1.0	9.5±0.5	13.7±0.7	18.2±0.5
OBC (ICLR2023)	40.5±2.1	46.4±1.6	53.4±2.3	22.1±0.6	24.0±1.3	26.3±1.0	16.4±1.4	19.5±1.5	21.6±1.4	9.6±0.5	11.4±0.9	14.6±1.1
OnPro (ICCV2023)	<u>46.0±1.6</u>	<u>52.9±2.0</u>	<u>59.5±0.7</u>	17.4±0.8	19.4±0.4	21.6±0.6	13.7±0.9	16.8±0.7	18.1±1.1	10.2±0.8	13.6±0.7	16.5±0.4
UER (ACMMM2023)	41.5±1.4	49.2±1.7	55.8±1.9	<u>24.6±0.8</u>	<u>27.0±0.5</u>	<u>29.6±1.1</u>	<u>21.9±1.3</u>	<u>25.1±1.1</u>	<u>27.5±1.1</u>	10.6±0.5	13.8±0.7	17.2±0.6
PCR (Algorithm (1))	45.4±1.3	50.3±1.5	56.0±1.2	25.6±0.6	27.4±0.6	29.3±1.1	24.2±0.9	27.2±1.2	28.4±0.9	12.2±0.9	17.4±0.7	19.6±0.8
HPCR (Algorithm (2))	48.3±1.5	53.4±1.4	60.1±1.1	29.1±0.7	30.7±0.5	33.7±0.6	27.1±0.6	29.9±0.7	31.3±0.7	16.4±0.3	19.5±0.8	22.1±0.5

TABLE 4

Final Accuracy Rate (higher is better) on Split CIFAR100 under the experimental setting of [7].

Buffer	1000	2000	5000
SCR [7]	26.5±0.2	31.6±0.5	36.5±0.2
OCM [7]	28.1±0.3	35.0±0.4	42.4±0.5
OnPro [62]	30.0±0.4	35.9±0.6	42.7±0.9
PCR	29.3±0.6	36.3±0.9	46.5±0.8
HPCR	33.6±0.6	40.5±1.5	49.1±1.2

at the i th task based on $a_{i,j}$ ($j \leq i$). If the model finishes all of T tasks, A_T is equivalent to the final accuracy rate.

6.1.4 Implementation Details

The basic setting of the backbone is the same as the recent work [12]. In detail, we take the Reduced ResNet18 (the number of filters is 20) as the feature extractor for all datasets. The classifier is NCM classifier for SCR and softmax classifier for other methods. During the training phase, the network, which is randomly initialized rather than pre-trained, is trained with the SGD optimizer, and the learning rate is set as 0.1.

For all datasets, the classes are shuffled before division. And we set the memory buffer with different sizes for all datasets. The model receives 10 current samples from the data stream and 10 previous samples from the memory buffer at a time irrespective of the size of the memory. Moreover, we employ a combination of various augmentation techniques to get the augmented images. And the usage of data augmentation is fair for all methods. For example, 10 original samples can produce 10 augmented samples, hence the number of forward passes in SCR is actually 20. To be fair, we concatenate 10 original samples and 10 augmented samples into a new batch containing 20 samples for other methods. With regard to hyperparameters of PCR, we select them on a validation set that is obtained by sampling 10% of the training set. As for the testing phase, we set 256 as the batch size of validation.

6.2 Overall Performance

In this section, we conduct experiments to compare with various state-of-the-art baselines of continual learning. Table 3 shows the final accuracy rate for Split CIFAR10, Split CIFAR100, Split MiniImageNet, and Split TinyImageNet. All reported scores are the average score of 10 runs with 95% confidence interval. Overall, our methods obtain significantly improved performance on four datasets.

Comparison on final accuracy. Table 3 reports the final accuracy of all evaluated methods on four datasets. By comparing the final accuracy of all methods, we can draw two conclusions. First, the model update strategies are more effective and can greatly improve the performance among all replay-based methods. Second, UER, OnPro, and ER-ACE are all good performing methods among all baselines.

The overall performance of PCR is advanced compared to all baselines, conclusively validating its remarkable effectiveness to publish in [13]. Notably, among the four datasets, PCR exhibits unparalleled prowess on Split CIFAR100 and Split MiniImageNet. Furthermore, as the memory buffer size grows, the performance of PCR continues to grow. For instance, PCR showcases striking improvements of more than 10% over the proxy-based baseline ER and the contrastive-based baseline SCR. Impressively, when the size of the memory buffer reaches 1000, 2000, and 5000, PCR surpasses ER-ACE, achieving performance boosts of 2.5%, 2.6%, and 2.3% on Split CIFAR100, respectively. Similarly, in the challenging context of Split MiniImageNet, PCR emerges victorious with substantial enhancements. With memory buffer sizes of 1000, 2000, and 5000, PCR outperforms UER by 2.3%, 2.2%, and 0.9%, respectively, further cementing its superiority. These outstanding results firmly establish PCR as the advanced replay-based method, underscoring its potential to drive progress in OCL.

Simultaneously, the enhanced method proposed in this work, HPCR, has consistently achieved the best performance compared to all baseline methods. In a multitude

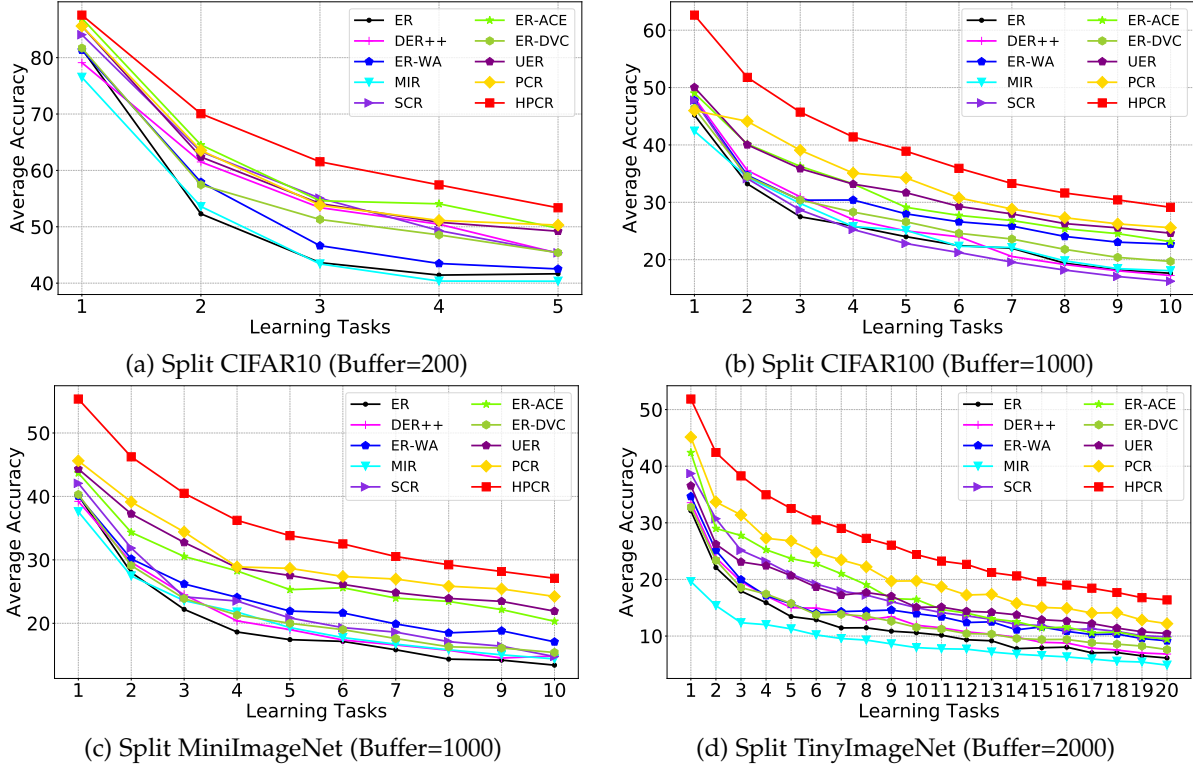


Fig. 4. Average accuracy rate on observed learning stages on all datasets.

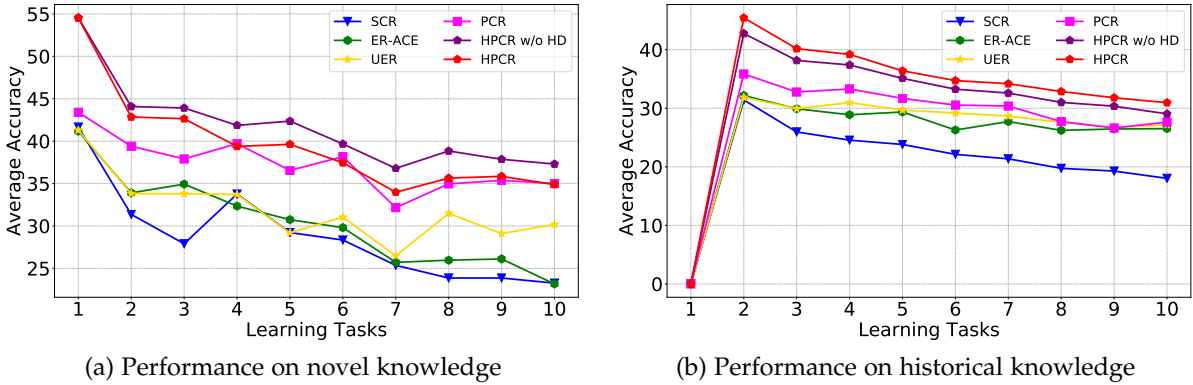


Fig. 5. Average accuracy rate on observed learning stages Split MiniImageNet while the buffer size is 5000.

of experimental scenarios, where each dataset comprises four memory buffers of varying sizes, HPCR consistently outshines all other methods. In particular, it exhibits even more remarkable performance compared to PCR. Specifically, HPCR shows a significant advancement, incorporating contrastive, temperature, and distillation components to further refine the PCR framework. For instance, on Split Cifar10, HPCR outperforms PCR by noteworthy margins of 2.9%, 3.1%, and 4.1% for memory buffer sizes of 100, 200, and 500, respectively. Additionally, on Split MiniImageNet, HPCR achieves remarkable improvements over PCR with significant gaps of 4.2%, 2.1%, and 2.7% for memory buffer sizes of 2000, 4000, and 5000, respectively. These compelling results unequivocally highlight the crucial significance of the components introduced in this article, as they play a pivotal role in elevating the performance of PCR. The integration of three components brings about substantial improvements, firmly establishing HPCR as a powerful and cutting-edge replay-based method in OCL.

Moreover, we conduct a comprehensive comparative analysis between SCR, OCM, OnPro, PCR, and HPCR, utilizing the experimental setup outlined in [7]. In this particular study, the model is configured as ResNet18 with 64 filters, and 64 samples are retrieved from the memory buffer for each training batch. The training process employs the Adam optimizer with a learning rate 0.001. It is important to note that these experimental conditions differ from those employed in our own study. As presented in Table 4, our methods (PCR and HPCR) demonstrate remarkable superiority over SCR, OCM, and OnPro under different experimental settings. This evidence further reinforces the effectiveness and robustness of our methods in comparison to existing approaches.

Comparison on learning process. For a more detailed comparison, we also report the accuracy in each learning task for part of effective approaches on four datasets, as shown in Figure 4. The results reflect the performance of all methods during the learning process, which can further

TABLE 5
Final Accuracy Rate (higher is better) on three datasets for ablation studies. ER acts as a baseline method.

Datasets	Split CIFAR10			Split CIFAR100			Split MiniImageNet			Split TinyImageNet		
Buffer	100	200	500	1000	2000	5000	1000	2000	5000	2000	4000	10000
ER	33.8 \pm 3.2	41.7 \pm 2.8	46.0 \pm 3.5	17.6 \pm 0.9	19.7 \pm 1.6	20.9 \pm 1.2	13.4 \pm 0.9	16.5 \pm 0.9	16.2 \pm 1.7	6.1 \pm 0.5	8.5 \pm 0.7	8.9 \pm 0.6
Couple (Equation 10)	38.4 \pm 3.0	43.2 \pm 3.8	49.1 \pm 3.9	17.9 \pm 0.8	19.7 \pm 0.8	21.6 \pm 1.0	17.9 \pm 0.7	19.9 \pm 0.8	20.9 \pm 1.6	5.2 \pm 0.4	10.7 \pm 0.7	12.8 \pm 0.5
Couple (Equation 11)	34.1 \pm 2.3	41.8 \pm 3.9	46.3 \pm 2.8	18.7 \pm 0.9	20.7 \pm 0.8	21.8 \pm 0.9	16.3 \pm 0.8	18.7 \pm 0.7	19.8 \pm 0.9	6.2 \pm 0.3	10.1 \pm 0.6	11.0 \pm 0.8
ER+PS	39.4 \pm 3.2	48.8 \pm 1.1	52.3 \pm 1.7	25.5 \pm 0.6	26.0 \pm 0.7	28.2 \pm 0.7	22.8 \pm 0.8	25.6 \pm 1.1	27.5 \pm 1.0	11.7 \pm 0.8	15.7 \pm 1.1	18.5 \pm 0.7
ER+PS+PD (PCR)	45.4 \pm 1.3	50.3 \pm 1.5	56.0 \pm 1.2	25.6 \pm 0.6	27.4 \pm 0.6	29.3 \pm 1.1	24.2 \pm 0.9	27.2 \pm 1.2	28.4 \pm 0.9	12.2 \pm 0.9	17.4 \pm 0.7	19.6 \pm 0.8
ER+PS+PD+PC	43.7 \pm 1.2	49.1 \pm 1.3	56.2 \pm 1.2	26.0 \pm 0.4	28.2 \pm 0.6	30.1 \pm 1.0	23.5 \pm 0.6	26.8 \pm 0.5	28.0 \pm 0.6	13.0 \pm 0.4	17.2 \pm 0.4	19.5 \pm 0.6
PCR+HC (PCR _C)	41.9 \pm 2.0	48.3 \pm 2.4	55.8 \pm 1.2	24.1 \pm 0.5	25.9 \pm 0.5	27.3 \pm 0.7	21.8 \pm 0.8	24.5 \pm 0.9	26.3 \pm 1.0	11.1 \pm 1.2	13.6 \pm 0.7	15.3 \pm 1.2
PCR+HC+HT (PCR _{CT})	47.4 \pm 2.2	51.3 \pm 1.6	57.7 \pm 1.1	27.2 \pm 0.5	29.3 \pm 0.7	31.6 \pm 0.9	25.6 \pm 1.0	28.5 \pm 0.5	29.8 \pm 0.7	14.8 \pm 0.6	18.8 \pm 0.5	20.8 \pm 0.5
PCR _{CT} +PCD	48.0 \pm 1.9	52.4 \pm 1.2	59.1 \pm 1.2	28.6 \pm 0.8	30.1 \pm 0.7	33.0 \pm 0.5	26.6 \pm 0.5	29.3 \pm 0.6	30.9 \pm 0.7	15.6 \pm 0.3	19.2 \pm 0.5	21.8 \pm 0.6
PCR _{CT} +PCD+SCD (HPCR)	48.3 \pm 1.5	53.4 \pm 1.4	60.1 \pm 1.1	29.1 \pm 0.7	30.7 \pm 0.5	33.7 \pm 0.6	27.1 \pm 0.6	29.9 \pm 0.7	31.3 \pm 0.7	16.4 \pm 0.3	19.5 \pm 0.8	22.1 \pm 0.5

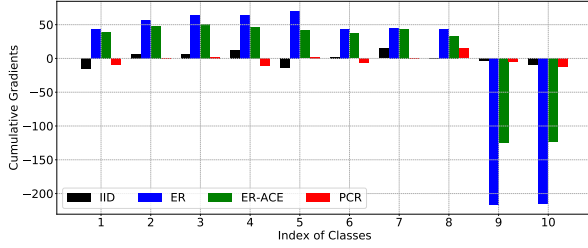


Fig. 6. Cumulative gradient of different methods for all proxies when the model learns new classes (9/10) on Split CIFAR10.

validate the overall performance of the methods. The results of the line chart show that PCR and HPCR not only achieve significant results in the accuracy of the final task, but also perform better than other baselines during the whole learning process. Meanwhile, the performance of PCR in the first few tasks does not outperform other baselines. However, its improvement becomes more and more visible as the number of tasks increases, proving its power to overcome CF. For instance, PCR does not perform best in the first task, but it demonstrates outstanding advantages in the remaining tasks on Split CIFAR100. Fortunately, this issue has been resolved in HPCR. Compared with the red and orange lines, HPCR still performs well in the first few tasks. Therefore, our approaches have a stronger ability to resist forgetting.

Comparison on knowledge balance. Actually, we should not only focus on the model’s ability to retain historical knowledge, but also ensure the model’s ability to quickly learn novel knowledge. Shown in Figure 5, we record the accuracy performance of novel and historical knowledge in each task for part of effective methods on Split MiniImageNet. Although SCR, ER-ACE, and UER can improve the anti-forgetting ability of the model, they tend to limit the generalization ability of the model. As the historical knowledge is consolidated, the learning performance of the model on novel knowledge becomes very poor. Different from existing studies, our model can not only effectively alleviate the phenomenon of CF, but also reduce the decline of the model at the generalization level as much as possible. Compared with HPCR (red line) and PCR (orange line), it is not difficult to find that there is a significant improvement in the memory ability of old knowledge.

6.3 Ablation Study

In this section, we decompose HPCR into several components and further demonstrate their functions. We conduct

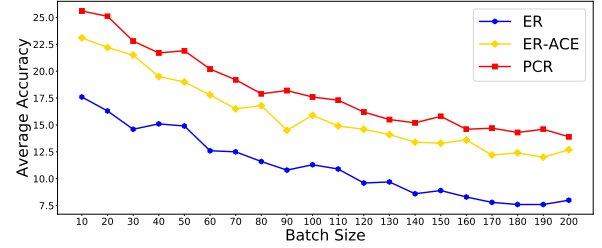


Fig. 7. Final accuracy rate (higher is better) on Split CIFAR100 with different batch sizes when the buffer size is 1000.

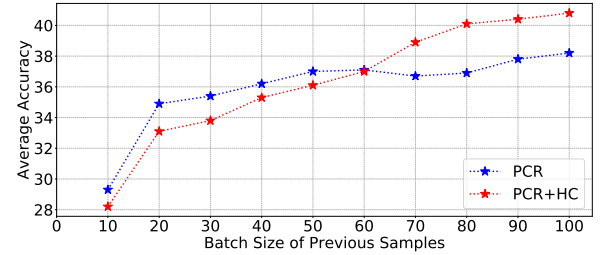


Fig. 8. Final Accuracy Rate (higher is better) on Split CIFAR100 (buffer size=1000) with different batch sizes of previous samples.

experiments on four datasets with different settings and record their final accuracy rate in Table 5. In addition to ER, we also include the two types of combination methods denoted as Equation (10) and Equation (11). The experimental results show that these two combination methods are not significant since they do not solve the problem of forgetting.

6.3.1 The Components of PCR

The **selection component** (PS) is the basic component of PCR, which selects the anchor-to-proxy pairs in the contrastive-based replay manner. Actually, there are some samples from the same classes in a training batch. As a result, there are some duplicate anchor-to-proxy pairs in PCR. To effectively verify the role of the selected proxies, we remove the duplicate pairs. As shown in Table 5, the performance of ER is significantly improved with the help of this component.

The other component of PCR is a **duplication component** (PD) to keep the duplicate pairs in PCR. Although it contains the same knowledge as the anchor-to-proxy pairs in the selection component, it still produces significant performance. Since it can provide anchor samples with more negative pairs, which are vital to contrastive-based loss. As described by the gradient analysis of PCR in Section 4, the number of duplicate pairs will be used as the weight of pairs

TABLE 6
Analysis results on CIFAR10 (buffer size=100) with and without temperature component.

Different Setting	Final Accuracy	Cumulative gradient	Loss	Difference (all classes)	Difference (new classes)
w/o HT	42.83	88.27/-95.39	1.8439	0.0042	0.0056
with HT	47.66	64.28/-70.40	1.6710	0.0025	0.0040

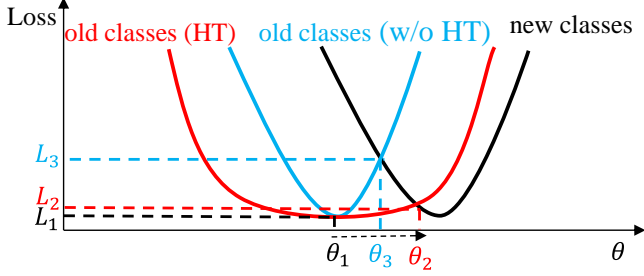


Fig. 9. Illustration of a steep region not using HT and a flat region using HT in the parameter space.

for the probability distribution calculation of the sample. This weight not only reduces the negative gradient of the current sample towards other classes, but also increases the positive gradient of a previous sample towards its class. As stated in Table 5, PCR outperforms “ER+PS” with the duplication component PD.

The **classifier component** (PC), which replaces the original softmax classifier by NCM classifier for PCR, is a less important part. Before testing, the NCM classifier requires recalculating the feature vectors of previous samples in the buffer to obtain the final classifier. Compared to the original classifier, it requires additional time and operation, which is unfavorable for OCL. As demonstrated in Table 5, the combination of PCR and NCM classifier is not necessarily the best. And NCM classifier is more suitable for situations with smaller samples (e.g. Split-CIFAR100) and a larger buffer. Since small-sized samples are easy to obtain reliable features, and large-sized buffer trends to obtain accurate classification centers.

In conclusion, the selection component and the duplication component are the keys of PCR. As displayed in Figure 6, PCR produces uniform gradients for all proxies to address the “bias” issue by the smart selection of anchor-to-proxy pairs. Furthermore, since the way of selection depends on the classes in the training batch, PCR is influenced by the batch size. Figure 7 reports the performance of several methods with different batch sizes. With the increase in batch size, PCR consistently maintains its advantages.

6.3.2 The Components of HPCR

Contrastive component (HC), which conditionally incorporates anchor-to-sample pairs to PCR, is the basic component of HPCR. Although it provides more knowledge about the relationships of samples, its performance is limited by a small batch size of training samples, as the “PCR+HC” indicated in Table 5. Moreover, we conduct experiments on Split CIFAR100 using PCR with and without HC when the buffer size is 5000. The results revealed in Figure 8 show that the anchor-to-sample pairs can reduce the performance of PCR when the batch size of the training samples is small (< 60), and vice versa. Hence, the usage of anchor-

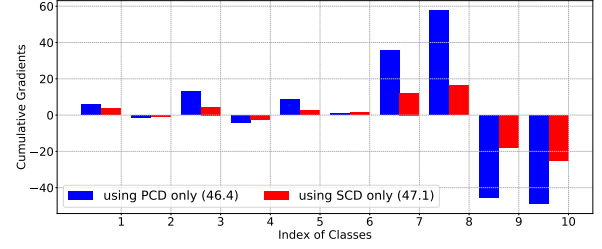


Fig. 10. Cumulative gradient for all proxies using different distillation loss functions when the model learns new classes (9/10) on Split CIFAR10.

TABLE 7
Accuracy Rate (higher is better) of HPCR on Split CIFAR100 with different τ_{min} and τ_{max} when the cycle length is 500.

$\tau_{min} \backslash \tau_{max}$	0.12	0.14	0.16	0.18	0.2
0.11	25.4, 34.9	25.0, 36.9	26.2, 36.6	26.3, 36.6	25.9, 36.7
0.09	25.5, 35.8	26.0, 36.7	26.1, 36.9	26.5, 37.6	26.1, 37.8
0.07	26.6, 36.8	26.3, 37.1	26.4, 37.6	26.2, 37.3	27.0, 38.1
0.05	26.6, 37.1	26.7, 37.7	27.7, 38.5	26.9, 37.9	26.5, 37.6

to-sample pairs should be conditional and controlled by a stage function, which is denoted as Equation (21).

Temperature component (HT) is to improve the generalization ability of the model. As stated in Table 5, with the help of HT, the performance of PCR is greatly improved. Compared with “PCR” and “PCR w/o HD” in Figure 5, we find that the main improvement brought by HT lies in the learning of novel knowledge by the model. To explore the role of HT, we analyze the training process of PCR on the CIFAR10 with and without HT, and some important indicators are recorded in Table 6. The results show the final accuracy can be improved by HT since the model can produce less gradient for old classes ($64.28 < 88.27$) and new classes ($70.40 < 90.39$). In the meantime, we find that the model reaches a place where the function value is relatively small ($1.6710 < 1.8439$) and the function surface is relatively flat during the optimization process. To validate it, we add uniformly distributed noise to the parameters of the final model, causing the position of the model to change in the parameter space. At the same time, we record the differences in training loss before and after the model changes. After repeating the above operations 1000 times, we calculate the average of these 1000 results. The results indicate that the model has relatively small differences using HT for all classes ($0.0025 < 0.0042$) and new classes ($0.0040 < 0.0056$). Therefore, the optimal solution of the model using HT is in a relatively flat region. As displayed in Figure 9, in such a flat region, the model, where the initial solution is θ_1 , can obtain a better solution θ_2 than θ_3 for both old and new classes. Moreover, The selection of hyperparameters related to Equation (23) is shown in Tables 7 and 8. And we set $\tau_{max} = 0.16$, $\tau_{min} = 0.05$, and $S = 500$ based on the results.

Distillation component (HD) is to improve the anti-forgetting ability of the model. Compared with “HPCR” and “HPCR w/o HD” in Figure 5, we can find that HPCR performs significantly better on historical knowledge with the help of HD. Shown as Table 5, the distillation component, which contains SCD and PCD, further improves the performance of PCR. To improve the overall performance of the model, both SCD and PCD are essential. For one

TABLE 8
Accuracy Rate (higher is better) of HPCR on Split CIFAR100 with different cycle lengths S .

S	50	100	125	250	500	1000
Final Accuracy	24.7	25.7	25.8	26.7	27.7	23.2
Averaged Accuracy	34.6	36.5	36.8	37.8	38.5	32.4

TABLE 9
Final Accuracy Rate (higher is better) of each task on Split CIFAR10 using distillation as DER or PCD.

Task	1	2	3	4	5	Average
DER [38]	0.3480	0.2205	0.4320	0.5315	0.7500	0.4564
PCD (ours)	0.3695	0.2270	0.488	0.4960	0.7405	0.4642

thing, SCD can better balance the distribution of historical knowledge while improving the model’s ability to anti-forgetting. Actually, there is an imbalance between old classes in OCL. As shown in Table 9, although tasks 1-4 are all old tasks, the performance of the model on these tasks is different. Compared with the distillation method in DER, PCD can better balance the performance of the model on old tasks (Tasks 1-4). For another thing, SCD, which directly propagates gradient for feature extractor, can produce less gradient for all proxies than PCD. As shown in Figure 10, if HPCR only uses SCD, the gradient it produces is relatively small, and the final performance is also better.

In summary, based on these three components, HPCR has a comprehensive improvement compared to PCR. At the same time, all of the components are tailored to break the limitations of PCR, and have their own originality.

6.4 Other Study

Visualization of Embedding. Visualization can help reflect the role of these components more intuitively. We train the model by ER and HPCR on Split CIFAR10 with 500 sizes of memory buffer, respectively. At the end of the training, we report their 2D t-SNE [77] visualization of feature embeddings for all testing samples, as shown in Figure 11. The stars are proxies while others are samples for all classes. The results demonstrate that HPCR not only achieves great performance, but also can indeed improve the distinguishability of samples in the embedding space.

Computation and Memory Budget. For OCL, the overhead of memory and computing resources is crucial, since it will affect the practicality of a method. Therefore, we analyze the memory and computational cost of different methods, as reported in Table 10. 1) Similar to [78], we use C_D to compare the computation of different methods. The C_D is denoted as a relative complexity between the stream and an underlying continual learning method. For example, when current samples come, ER can immediately learn them and then predict unknown samples, resulting in a relative complexity of 1. Since UER, ER-ACE, PCR, and HPCR only modify the loss objective of ER, their computational complexities are equivalent to 1. However, OCM and OnPro require an additional 16 augmentation to the original data, making it require 16 times the FLOPs needed by ER. Thus, its computational complexity is 16, which limits the ability of real-time prediction. 2) We set the memory budget of the model for ER as 1. Due to the OCM method requiring an additional model to be saved for knowledge distillation,

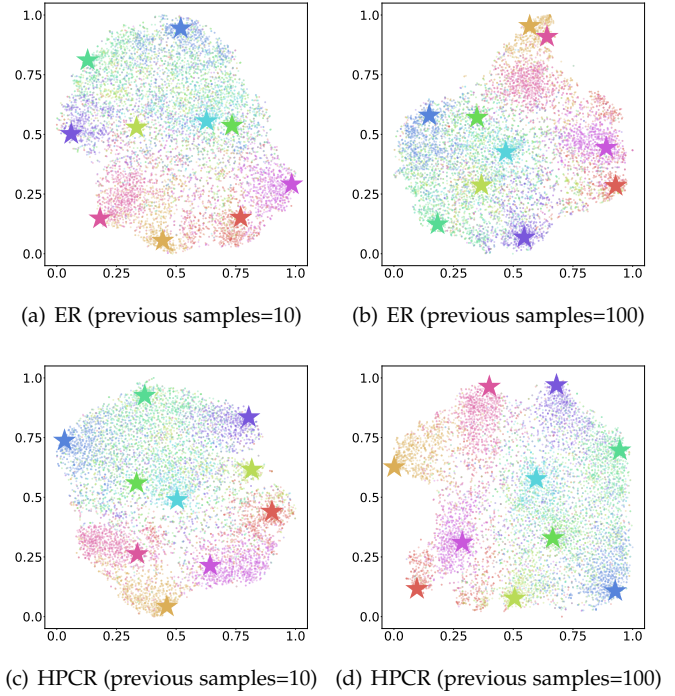


Fig. 11. 2D t-SNE visualization of feature embeddings for the testing samples at the end of the training on Split CIFAR10 (buffer size=500).

TABLE 10
The computation and memory budget of different methods.

Method	ER	ER-ACE	OCM	OnPro	UER	PCR	HPCR
Computation (C_D)	1	1	16	16	1	1	1
Memory (Model)	1	1	2	1	1	1	1
Memory (Data)	1	1	1	1	1	1	1.25

its relative budget is 2 and others are 1. 3) We compare the data’s memory budget of various methods using the data size of all samples in the buffer. Due to the need for additional storage of the feature and logits embedding, HPCR requires more relative storage space (1.25 times that of other methods). Nevertheless, the performance improvement brought about by this additional space consumption is worth it. In a word, HPCR is a simple yet effective method for real-time prediction of OCL.

7 CONCLUSION

In this paper, we propose a novel OCL method called PCR to alleviate the phenomenon of catastrophic forgetting by the coupling of proxy-based and contrastive-based replay manners. PCR replaces the samples of anchor-to-sample pairs by proxies, realizing complementary advantages. Based on PCR, we further develop a more holistic OCL method named HPCR, which mainly consists of three components. The contrastive component conditionally introduces anchor-to-sample pairs to PCR, improving the feature extraction ability of PCR when the training batch size is large. The temperature component decouples the influence of temperature on gradients in two parts and effectively improves the generalization ability of the model. The distillation component improves the anti-forgetting ability of the model through PCD and SCD. Extensive experiments on four datasets demonstrate the superiority of our proposed methods over a large variety of state-of-the-art methods.

ACKNOWLEDGMENTS

This work was supported in part by National Nature Science Foundation of China (No. 62272130 and No. 62376072), Nature Science Program of Shenzhen (No. JCYJ20210324120208022 and No. JCYJ20200109113014456), and Shenzhen Science and Technology Program (No. KCXFZ20211020163403005).

REFERENCES

- [1] L. Wang, X. Zhang, H. Su, and J. Zhu, "A comprehensive survey of continual learning: Theory, method and application," *arXiv preprint arXiv:2302.00487*, 2023. **1**
- [2] M. Masana, X. Liu, B. Twardowski, M. Menta, A. D. Bagdanov, and J. van de Weijer, "Class-incremental learning: survey and performance evaluation on image classification," *IEEE Transactions on Pattern Analysis and Machine Intelligence*, 2022. **1, 3**
- [3] Z. Li and D. Hoiem, "Learning without forgetting," *IEEE transactions on pattern analysis and machine intelligence*, vol. 40, no. 12, pp. 2935–2947, 2017. **1**
- [4] M. Boschini, L. Bonicelli, P. Buzzega, A. Porrello, and S. Calderara, "Class-incremental continual learning into the extended derive," *IEEE Transactions on Pattern Analysis and Machine Intelligence*, 2022. **1**
- [5] M. Delange, R. Aljundi, M. Masana, S. Parisot, X. Jia, A. Leonardis, G. Slabaugh, and T. Tuytelaars, "A continual learning survey: Defying forgetting in classification tasks," *IEEE Transactions on Pattern Analysis and Machine Intelligence*, 2021. **1, 3**
- [6] Z. Mai, R. Li, J. Jeong, D. Quispe, H. Kim, and S. Sanner, "Online continual learning in image classification: An empirical survey," *Neurocomputing*, vol. 469, pp. 28–51, 2022. **1, 3**
- [7] Y. Guo, B. Liu, and D. Zhao, "Online continual learning through mutual information maximization," in *International Conference on Machine Learning*. PMLR, 2022, pp. 8109–8126. **1, 4, 10, 11, 12**
- [8] H. Lin, S. Feng, X. Li, W. Li, and Y. Ye, "Anchor assisted experience replay for online class-incremental learning," *IEEE Transactions on Circuits and Systems for Video Technology*, 2022. **1**
- [9] X. Yao, Y. Bai, X. Zhang, Y. Zhang, Q. Sun, R. Chen, R. Li, and B. Yu, "Pcl: Proxy-based contrastive learning for domain generalization," in *Proceedings of the IEEE/CVF Conference on Computer Vision and Pattern Recognition*, 2022, pp. 7097–7107. **1, 4, 6**
- [10] T. Mensink, J. Verbeek, F. Perronnin, and G. Csorba, "Distance-based image classification: Generalizing to new classes at near-zero cost," *IEEE transactions on pattern analysis and machine intelligence*, vol. 35, no. 11, pp. 2624–2637, 2013. **1**
- [11] H. Ahn, J. Kwak, S. Lim, H. Bang, H. Kim, and T. Moon, "Ssil: Separated softmax for incremental learning," in *Proceedings of the IEEE/CVF International Conference on Computer Vision*, 2021, pp. 844–853. **2, 5, 10**
- [12] L. Caccia, R. Aljundi, N. Asadi, T. Tuytelaars, J. Pineau, and E. Belilovsky, "New insights on reducing abrupt representation change in online continual learning," in *International Conference on Learning Representations*, 2021. **2, 4, 5, 10, 11**
- [13] H. Lin, B. Zhang, S. Feng, X. Li, and Y. Ye, "Pcr: Proxy-based contrastive replay for online class-incremental continual learning," in *Proceedings of the IEEE/CVF Conference on Computer Vision and Pattern Recognition (CVPR)*, June 2023, pp. 24 246–24 255. **2, 3, 11**
- [14] H. Hu, O. Sener, F. Sha, and V. Koltun, "Drinking from a firehose: Continual learning with web-scale natural language," *IEEE Transactions on Pattern Analysis and Machine Intelligence*, 2022. **3**
- [15] X. Zhang, D. Song, and D. Tao, "Hierarchical prototype networks for continual graph representation learning," *IEEE Transactions on Pattern Analysis and Machine Intelligence*, 2022. **3**
- [16] G. Yang, E. Fini, D. Xu, P. Rota, M. Ding, M. Nabi, X. Alamedd-Pineda, and E. Ricci, "Uncertainty-aware contrastive distillation for incremental semantic segmentation," *IEEE Transactions on Pattern Analysis and Machine Intelligence*, 2022. **3**
- [17] W. Zhang, D. Li, C. Ma, G. Zhai, X. Yang, and K. Ma, "Continual learning for blind image quality assessment," *IEEE Transactions on Pattern Analysis and Machine Intelligence*, 2022. **3**
- [18] Q. Pham, C. Liu, and H. Steven, "Continual normalization: Rethinking batch normalization for online continual learning," in *International Conference on Learning Representations*, 2021. **3**
- [19] S. I. Mirzadeh, M. Farajtabar, D. Gorur, R. Pascanu, and H. Ghasemzadeh, "Linear mode connectivity in multitask and continual learning," in *International Conference on Learning Representations*, 2020. **3**
- [20] A. Prabhu, P. H. Torr, and P. K. Dokania, "Gdumb: A simple approach that questions our progress in continual learning," in *European conference on computer vision*. Springer, 2020, pp. 524–540. **3**
- [21] E. Belouadah, A. Popescu, and I. Kanellos, "A comprehensive study of class incremental learning algorithms for visual tasks," *Neural Networks*, vol. 135, pp. 38–54, 2021. **3**
- [22] B. Yang, M. Lin, Y. Zhang, B. Liu, X. Liang, R. Ji, and Q. Ye, "Dynamic support network for few-shot class incremental learning," *IEEE Transactions on Pattern Analysis and Machine Intelligence*, 2022. **3**
- [23] D.-W. Zhou, H.-J. Ye, L. Ma, D. Xie, S. Pu, and D.-C. Zhan, "Few-shot class-incremental learning by sampling multi-phase tasks," *IEEE Transactions on Pattern Analysis and Machine Intelligence*, 2022. **3**
- [24] S.-A. Rebuffi, A. Kolesnikov, G. Sperl, and C. H. Lampert, "icarl: Incremental classifier and representation learning," in *Proceedings of the IEEE conference on Computer Vision and Pattern Recognition*, 2017, pp. 2001–2010. **3**
- [25] H. Koh, D. Kim, J.-W. Ha, and J. Choi, "Online continual learning on class incremental blurry task configuration with anytime inference," *arXiv preprint arXiv:2110.10031*, 2021. **3**
- [26] R. Aljundi, K. Kelchtermans, and T. Tuytelaars, "Task-free continual learning," in *Proceedings of the IEEE/CVF Conference on Computer Vision and Pattern Recognition*, 2019, pp. 11 254–11 263. **3**
- [27] J. Bang, H. Kim, Y. Yoo, J.-W. Ha, and J. Choi, "Rainbow memory: Continual learning with a memory of diverse samples," in *Proceedings of the IEEE/CVF Conference on Computer Vision and Pattern Recognition*, 2021, pp. 8218–8227. **3**
- [28] A. A. Rusu, N. C. Rabinowitz, G. Desjardins, H. Soyer, J. Kirkpatrick, K. Kavukcuoglu, R. Pascanu, and R. Hadsell, "Progressive neural networks," *arXiv preprint arXiv:1606.04671*, 2016. **3**
- [29] Z. Miao, Z. Wang, W. Chen, and Q. Qiu, "Continual learning with filter atom swapping," in *International Conference on Learning Representations*, 2021. **3**
- [30] J. Kirkpatrick, R. Pascanu, N. Rabinowitz, J. Veness, G. Desjardins, A. A. Rusu, K. Milan, J. Quan, T. Ramalho, A. Grabska-Barwinska et al., "Overcoming catastrophic forgetting in neural networks," *Proceedings of the national academy of sciences*, vol. 114, no. 13, pp. 3521–3526, 2017. **3**
- [31] P. Dhar, R. V. Singh, K.-C. Peng, Z. Wu, and R. Chellappa, "Learning without memorizing," in *Proceedings of the IEEE/CVF Conference on Computer Vision and Pattern Recognition*, 2019, pp. 5138–5146. **3**
- [32] G. Hinton, O. Vinyals, J. Dean et al., "Distilling the knowledge in a neural network," *arXiv preprint arXiv:1503.02531*, vol. 2, no. 7, 2015. **3, 9**
- [33] G. M. van de Ven, H. T. Siegelmann, and A. S. Tolias, "Brain-inspired replay for continual learning with artificial neural networks," *Nature communications*, vol. 11, no. 1, pp. 1–14, 2020. **3**
- [34] Y. Xiang, Y. Fu, P. Ji, and H. Huang, "Incremental learning using conditional adversarial networks," in *Proceedings of the IEEE/CVF International Conference on Computer Vision*, 2019, pp. 6619–6628. **3**
- [35] B. Cui, G. Hu, and S. Yu, "Deepcollaboration: Collaborative generative and discriminative models for class incremental learning," in *Proceedings of the AAAI Conference on Artificial Intelligence*, vol. 35, no. 2, 2021, pp. 1175–1183. **3**
- [36] Y. Choi, M. El-Khamy, and J. Lee, "Dual-teacher class-incremental learning with data-free generative replay," in *Proceedings of the IEEE/CVF Conference on Computer Vision and Pattern Recognition*, 2021, pp. 3543–3552. **3**
- [37] P. Buzzega, M. Boschini, A. Porrello, and S. Calderara, "Rethinking experience replay: a bag of tricks for continual learning," in *2020 25th International Conference on Pattern Recognition (ICPR)*. IEEE, 2021, pp. 2180–2187. **3**
- [38] P. Buzzega, M. Boschini, A. Porrello, D. Abati, and S. Calderara, "Dark experience for general continual learning: a strong, simple baseline," *Advances in neural information processing systems*, vol. 33, pp. 15 920–15 930, 2020. **3, 9, 10, 15**
- [39] H. Cha, J. Lee, and J. Shin, "Co2l: Contrastive continual learning," in *Proceedings of the IEEE/CVF International Conference on Computer Vision*, 2021, pp. 9516–9525. **3**

- [40] A. Chaudhry, A. Gordo, P. Dokania, P. Torr, and D. Lopez-Paz, "Using hindsight to anchor past knowledge in continual learning," in *Proceedings of the AAAI Conference on Artificial Intelligence*, vol. 35, no. 8, 2021, pp. 6993–7001. [3](#)
- [41] Y. Liu, B. Schiele, and Q. Sun, "Rmm: Reinforced memory management for class-incremental learning," *Advances in Neural Information Processing Systems*, vol. 34, 2021. [3](#)
- [42] L. Wang, X. Zhang, K. Yang, L. Yu, C. Li, H. Lanqing, S. Zhang, Z. Li, Y. Zhong, and J. Zhu, "Memory replay with data compression for continual learning," in *International Conference on Learning Representations*, 2021. [3](#)
- [43] D. Lopez-Paz and M. Ranzato, "Gradient episodic memory for continual learning," *Advances in neural information processing systems*, vol. 30, 2017. [3](#)
- [44] A. Chaudhry, M. Ranzato, M. Rohrbach, and M. Elhoseiny, "Efficient lifelong learning with a-gem," in *International Conference on Learning Representations*, 2018. [3](#), [10](#)
- [45] M. Farajtabar, N. Azizan, A. Mott, and A. Li, "Orthogonal gradient descent for continual learning," in *International Conference on Artificial Intelligence and Statistics*. PMLR, 2020, pp. 3762–3773. [3](#)
- [46] S. Tang, D. Chen, J. Zhu, S. Yu, and W. Ouyang, "Layerwise optimization by gradient decomposition for continual learning," in *Proceedings of the IEEE/CVF Conference on Computer Vision and Pattern Recognition*, 2021, pp. 9634–9643. [3](#)
- [47] Y. Guo, W. Hu, D. Zhao, and B. Liu, "Adaptive orthogonal projection for batch and online continual learning," *Proceedings of AAAI-2022*, vol. 2, 2022. [3](#)
- [48] F. Zhu, Z. Cheng, X.-y. Zhang, and C.-I. Liu, "Class-incremental learning via dual augmentation," *Advances in Neural Information Processing Systems*, vol. 34, 2021. [3](#)
- [49] D. Rolnick, A. Ahuja, J. Schwarz, T. Lillicrap, and G. Wayne, "Experience replay for continual learning," *Advances in Neural Information Processing Systems*, vol. 32, 2019. [3](#), [4](#), [10](#)
- [50] R. Aljundi, E. Belilovsky, T. Tuytelaars, L. Charlin, M. Caccia, M. Lin, and L. Page-Caccia, "Online continual learning with maximal interfered retrieval," *Advances in Neural Information Processing Systems*, vol. 32, pp. 11 849–11 860, 2019. [3](#), [10](#)
- [51] D. Shim, Z. Mai, J. Jeong, S. Sanner, H. Kim, and J. Jang, "Online class-incremental continual learning with adversarial shapley value," in *Proceedings of the AAAI Conference on Artificial Intelligence*, vol. 35, no. 11, 2021, pp. 9630–9638. [3](#), [10](#)
- [52] R. Aljundi, M. Lin, B. Goujaud, and Y. Bengio, "Gradient based sample selection for online continual learning," *Advances in neural information processing systems*, vol. 32, 2019. [3](#), [10](#)
- [53] X. Jin, A. Sadhu, J. Du, and X. Ren, "Gradient-based editing of memory examples for online task-free continual learning," *Advances in Neural Information Processing Systems*, vol. 34, 2021. [3](#), [10](#)
- [54] J. He and F. Zhu, "Online continual learning for visual food classification," in *Proceedings of the IEEE/CVF International Conference on Computer Vision*, 2021, pp. 2337–2346. [3](#)
- [55] Z. Wang, L. Shen, L. Fang, Q. Suo, T. Duan, and M. Gao, "Improving task-free continual learning by distributionally robust memory evolution," in *International Conference on Machine Learning*. PMLR, 2022, pp. 22 985–22 998. [3](#)
- [56] Z. Mai, R. Li, H. Kim, and S. Sanner, "Supervised contrastive replay: Revisiting the nearest class mean classifier in online class-incremental continual learning," in *Proceedings of the IEEE/CVF Conference on Computer Vision and Pattern Recognition*, 2021, pp. 3589–3599. [4](#), [5](#), [10](#)
- [57] H. Yin, P. Li *et al.*, "Mitigating forgetting in online continual learning with neuron calibration," *Advances in Neural Information Processing Systems*, vol. 34, 2021. [4](#)
- [58] Y. Gu, X. Yang, K. Wei, and C. Deng, "Not just selection, but exploration: Online class-incremental continual learning via dual view consistency," in *Proceedings of the IEEE/CVF Conference on Computer Vision and Pattern Recognition*, 2022, pp. 7442–7451. [4](#), [10](#)
- [59] A. Chrysakis and M.-F. Moens, "Online bias correction for task-free continual learning," in *The Eleventh International Conference on Learning Representations*. [4](#), [10](#)
- [60] Y. Zhang, B. Pfahringer, E. Frank, A. Bifet, N. J. S. Lim, and Y. Jia, "A simple but strong baseline for online continual learning: Repeated augmented rehearsal," *Advances in Neural Information Processing Systems*, vol. 35, pp. 14 771–14 783, 2022. [4](#)
- [61] H. Lin, S. Feng, B. Zhang, H. Qiao, X. Li, and Y. Ye, "Uer: A heuristic bias addressing approach for online continual learning," *arXiv preprint arXiv:2309.04081*, 2023. [4](#), [10](#)
- [62] Y. Wei, J. Ye, Z. Huang, J. Zhang, and H. Shan, "Online prototype learning for online continual learning," *arXiv preprint arXiv:2308.00301*, 2023. [4](#), [10](#), [11](#)
- [63] S. Kan, Z. He, Y. Cen, Y. Li, V. Mladenovic, and Z. He, "Contrastive bayesian analysis for deep metric learning," *IEEE Transactions on Pattern Analysis and Machine Intelligence*, 2022. [4](#)
- [64] T. Milbich, K. Roth, B. Brattoli, and B. Ommer, "Sharing matters for generalization in deep metric learning," *IEEE Transactions on Pattern Analysis and Machine Intelligence*, vol. 44, no. 1, pp. 416–427, 2020. [4](#)
- [65] J. Lim, S. Yun, S. Park, and J. Y. Choi, "Hypergraph-induced semantic tuple loss for deep metric learning," in *Proceedings of the IEEE/CVF Conference on Computer Vision and Pattern Recognition*, 2022, pp. 212–222. [4](#)
- [66] W. Zhao, Y. Rao, Z. Wang, J. Lu, and J. Zhou, "Towards interpretable deep metric learning with structural matching," in *Proceedings of the IEEE/CVF International Conference on Computer Vision*, 2021, pp. 9887–9896. [4](#)
- [67] I. Elezi, J. Seidenschwarz, L. Wagner, S. Vascon, A. Torcinovich, M. Pelillo, and L. Leal-Taixe, "The group loss++: A deeper look into group loss for deep metric learning," *IEEE Transactions on Pattern Analysis and Machine Intelligence*, 2022. [4](#)
- [68] W. Zheng, J. Lu, and J. Zhou, "Deep metric learning with adaptively composite dynamic constraints," *IEEE Transactions on Pattern Analysis and Machine Intelligence*, 2023. [4](#)
- [69] K. Roth, O. Vinyals, and Z. Akata, "Non-isotropy regularization for proxy-based deep metric learning," in *Proceedings of the IEEE/CVF Conference on Computer Vision and Pattern Recognition*, 2022, pp. 7420–7430. [4](#)
- [70] S. Hou, X. Pan, C. C. Loy, Z. Wang, and D. Lin, "Learning a unified classifier incrementally via rebalancing," in *Proceedings of the IEEE/CVF Conference on Computer Vision and Pattern Recognition*, 2019, pp. 831–839. [4](#), [8](#)
- [71] T. Li, P. Cao, Y. Yuan, L. Fan, Y. Yang, R. S. Feris, P. Indyk, and D. Katabi, "Targeted supervised contrastive learning for long-tailed recognition," in *Proceedings of the IEEE/CVF Conference on Computer Vision and Pattern Recognition*, 2022, pp. 6918–6928. [6](#)
- [72] F. Wang and H. Liu, "Understanding the behaviour of contrastive loss," in *Proceedings of the IEEE/CVF conference on computer vision and pattern recognition*, 2021, pp. 2495–2504. [8](#)
- [73] A. Krizhevsky, G. Hinton *et al.*, "Learning multiple layers of features from tiny images," 2009. [10](#)
- [74] O. Vinyals, C. Blundell, T. Lillicrap, D. Wierstra *et al.*, "Matching networks for one shot learning," *Advances in neural information processing systems*, vol. 29, pp. 3630–3638, 2016. [10](#)
- [75] Y. Le and X. Yang, "Tiny imagenet visual recognition challenge," *CS 231N*, vol. 7, no. 7, p. 3, 2015. [10](#)
- [76] B. Zhao, X. Xiao, G. Gan, B. Zhang, and S.-T. Xia, "Maintaining discrimination and fairness in class incremental learning," in *Proceedings of the IEEE/CVF Conference on Computer Vision and Pattern Recognition*, 2020, pp. 13 208–13 217. [10](#)
- [77] L. Van der Maaten and G. Hinton, "Visualizing data using t-sne," *Journal of machine learning research*, vol. 9, no. 11, 2008. [15](#)
- [78] Y. Ghunaim, A. Bibi, K. Alhamoud, M. Alfarrar, H. A. A. K. Hammoud, A. Prabhu, P. H. Torr, and B. Ghanem, "Real-time evaluation in online continual learning: A new paradigm," *arXiv preprint arXiv:2302.01047*, 2023. [15](#)



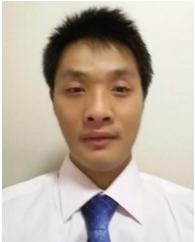
Huiwei Lin (Graduate Student Member, IEEE) is currently pursuing the Ph.D. degree with the School of Computer Science and Technology, Harbin Institute of Technology, Shenzhen, China. He received the B.S. degree from the South China University of Technology, China, in 2017, and the M.S. degree from the Harbin Institute of Technology, Shenzhen, China, in 2020. His current research interests include continual learning and time series analysis.



Shanshan Feng is currently a senior research scientist at the Centre for Frontier AI Research, Institute of High Performance Computing, the Agency for Science, Technology and Research (A*STAR), Singapore. He received the Ph.D. degree from Nanyang Technological University, Singapore in 2017, and his B.S. degree from University of Science and Technology of China in 2011. His current research interests include spatial-temporal data mining, social graph learning, and recommender systems.



Baoquan Zhang is currently an assistant professor with the School of Computer Science and Technology, Harbin Institute of Technology, Shenzhen. He received the B.S. degree from the Harbin Institute of Technology, Weihai, China, in 2015, the M.S. degree from the Harbin Institute of Technology, Harbin, China, in 2017, and the Ph.D. degree from the Harbin Institute of Technology, Shenzhen, in 2023. His current research interests include meta learning, few-shot learning, machine learning, and data mining.



Xutao Li is currently a Professor with the School of Computer Science and Technology, Harbin Institute of Technology, Shenzhen, China. He received the Ph.D. and Master degrees in Computer Science from Harbin Institute of Technology in 2013 and 2009, and the Bachelor from Lanzhou University of Technology in 2007. His research interests include data mining, machine learning, graph mining, and social network analysis, especially tensor-based learning, and mining algorithms.



Yew-soon Ong (Fellow, IEEE) received the PhD degree from the University of Southampton, U.K., in 2003. He is president's chair professor in Computer Science with Nanyang Technological University (NTU), and holds the position of chief artificial intelligence scientist of A*STAR, Singapore. At NTU, he serves as co-director of the Singtel-NTU Cognitive & Artificial Intelligence Joint Lab. His research interest is in artificial and computational intelligence. He is founding EIC of IEEE Transactions on Emerging Topics in Computational Intelligence and AE of IEEE Transactions on Neural Networks and Learning Systems, IEEE on Transactions on Cybernetics, IEEE Transactions on Artificial Intelligence and others. He has received several IEEE outstanding paper awards and was listed as a Thomson Reuters highly cited Researcher and among the World's Most Influential Scientific Minds.



Yunming Ye is currently a Professor with the School of Computer Science and Technology, Harbin Institute of Technology, Shenzhen, China. He received the PhD degree in Computer Science from Shanghai Jiao Tong University, Shanghai, China, in 2004. His research interests include data mining, text mining, and ensemble learning algorithms.